IQ Demodulator for DC Coupled Doppler Radar

A THESIS SUBMITTED TO THE GRADUATE DIVISION OF THE UNIVERSITY OF HAWAI‘I IN PARTIAL FULFILLMENT OF THE REQUIREMENTS FOR THE DEGREE OF

MASTER OF SCIENCE

IN

ELECTRICAL ENGINEERING

Dec 2010

By

Xi Zhao

Thesis Committee:

Olga Boric-Lubecke Chairperson

Victor M. Lubecke

David Garmire

ACKNOWLEDGMENTS

This work would not have been done without the valuable instructions of my thesis advisor, Dr. Olga Boric-Lubecke. I really appreciate her patience and encouragement in the past three years. My sincere gratitude is extended to Dr. Victor Lubecke and Dr. David Garmire for serving on my thesis committee.

I also would like to thank all my colleagues. Adiya Singh , Noah Hafner, Chenyan Song, Soumya Vinod, Xiaoxiao Zhang, Ehsaneh Shahhaidar, Wenqi Hu, and Xihang Cao, thank you for the generous help, very useful discussion, and moral support. The time spend with you in UHM will be the most precious treasure in my life.

I would like to express my appreciation to my parents and my boyfriend, Yichi Xu, for their love, understanding, and encouragement. Without their continuous support, it would not be possible for me to finish this degree.

ABSTRACT

The work in this thesis demonstrates the possibility of using DC coupled signal in Doppler radar systems. The microwave radar system can detect the periodic motion which can extend to the cardiopulmonary activity of human beings. One of the challenges in Doppler radar systems for physiological monitoring is a large DC offset in the baseband outputs. This DC offset is largely resulting from the parasitic signal leakage between radar ports. Since the physiological signals of interest include frequency content near DC, it is not desirable to simply AC couple radar outputs. While AC coupling effectively removes DC offset, it also introduces a large time delay and distortion. This thesis present the first DC coupled Doppler radar design and measurements. The DC coupling is achieved by using a mixer with high LO to RF port isolation, resulting in very low radar DC offset, on the order of mW. The printed circuit board (PCB) quadrature (IQ) demodulator was designed and fabricated using the high isolation mixers. The IQ demodulator was tested in the radar system to detect the motion of the moving target. DC offset in radar system was analyzed and measured. Two quadrature radar systems were tested for comparison (PCB system and coaxial system). Due to the lower LO leakage in the PCB system, significantly reduced DC offset was measured for both I and Q channels. The DC coupled signals from the PCB radar system were successfully detected before saturation of LNA. The DC coupled and AC coupled data were compared. The DC coupled results show great advantages of less signal distortion and more accurate rate estimation. This is the first reported DC coupled Doppler radar measurement result.

Table of Contents

List of Figures

Figure Page

List of Tables

Table Page

CHAPTER 1

INTRODUCTION

In recent years there has been an explosion in RF and wireless applications of all kinds, including cellular communications, wireless LAN, wireless sensor networks, and even wireless power. Increasingly sophisticated consumer demand and large market size have dictated and enabled hardware development to provide lower cost, smaller size, higher performance, and multi-tasking capability. These advances driven by progress in wireless systems can be applied to biomedical engineering and medical practice through the production of high performance medical equipment, particularly for addressing outpatient and chronic healthcare demands fueled by an aging population. One promising new technology which exploits developments in wireless and computational technologies is Doppler-radar for remote sensing of cardiopulmonary activity, which has great potential for continuous, remote health monitoring and personnel detection.

A Doppler radar is a specialized radar that makes use of the Doppler effect to detect velocity of moving objects at a distance. This is accomplished by sending a microwave signal towards a target of interest and listening for its reflection, then analyzing how the frequency of the returned signal has been altered by the object's motion. This variation gives direct and highly accurate measurements of the radial component of a target's velocity relative to the radar. Doppler radars are used in aviation, sounding satellites, police speed guns, and radiology. By applying the same sensing techniques for medical

applications, small motions of the human body caused by cardiopulmonary activity can be measured by a Doppler radar aimed at the human subject. A Continuous Wave microwave signal is transmitted towards the body and partly reflected back to the transmitter antenna. The received signal is compared to the transmit signal and the phase difference is a measure of the physiological motion of the subject. Applications of Microwave Doppler radar systems include medical equipment for patients who have a heart disease or sleep apnea syndrome, baby monitoring in order to avoid sudden infant death syndrome (SIDS), disaster rescue where the system can detect cardiopulmonary signals from people trapped in debris, and sense through the wall military applications.

Direct-conversion trasceivers are commonly used in wireless communications to avoid image rejection filters, and enable higher level of integration with lower power dissipation. Direct conversion radio architecture is also commonly used for microwave Doppler-radar non-contact cardiopulmonary monitoring. However, there are a number of challenges in direct conversion systems. Performance limitations typically stem from quadrature channel imbalance, LO leakage, DC offset and Flicker noise which affect the sensitivity of the radar system. Typically, CW radar output is AC coupled to eliminate large DC offsets resulting from LO leakage and clutter reflection. But for the biological signals with spectrum extending to near DC frequency, it is challenging to separate wanted information from DC components using a high pass filter. In this case AC coupling will result in signal distortion which affects the measurement accuracy. Due to the large DC offset, it is impractical to record the reasonable resolution data before amplifier saturation. In this project, a quadrature radar receiver printed circuit board was

designed to achieve low DC offset to enable DC coupling of Doppler radar output signals. The following chapters will provide radar background; describe IQ demodulator design, and present experimental data. The Chapter 2 introduces radar theory. The basic radar system and radar types are described, including Doppler radar. In Chapter 3, RF front-end architecture of Doppler radar is discussed, including single channel and quadrature systems. The design needs for building the IQ demodulator printed circuit board are discussed as well. In Chapter 4, the design, implementation and preliminary testing of the printed circuit IQ demodulator are presented. The DC offset in the radar system was discussed and measured in Chapter 5. Due to the very small DC offset in the PCB IQ demodulator system, the DC coupled signals were successfully digitized without amplifier saturation. A coaxial radar system was tested for comparison, and it was demonstrated that a low DC offset IQ demodulator provides significant performance gains. Finally Chapter 6 provides the conclusion, and outlines challenges for future work.

CHAPTER 2

DOPPLER RADAR THEORY

2.1 Radar Introduction

Radar (Radio Detection and Ranging) is a device that sends out electromagnetic waves. These waves reflect off of objects in space, and a proportion of the original wave energy is reflected back towards the radar. The radar then receives and analyzes this return signal. This return signal can be processed to determine many properties of the object that the wave reflected off of. For examples, the location of the objects (distance away from the radar) can be determined by the time delay between sent and returned signals; the velocity of the targets can be calculated from the frequency shift of the returned signal; the target's radar cross section (target's ability to reflect radar signals) can be analyzed by the strength of the signals, to determine target size, shape, and orientation.

A basic radar system consists of a transmitter, switch, antenna, receiver, data recorder, processor, and some sort of output display. In a pulsed radar, the transmitter transmits a high power pulse to a switch which then directs the pulse to be transmitted out an antenna. Just after the antenna is finished transmitting the pulse, the switch switches control to the receiver which allows the antenna to receive echoed signals. Once the signals are received the switch then transfers control back to the transmitter to transmit another signal. The switch may toggle control between the transmitter and the receiver

as much as 1000 times per second. The received signals must be processed to provide useful data.

In a radar system, the propagation properties of electromagnetic waves are advantageous for operation in air. Sound waves and ocean waves require matter to transport energy but EM waves can do so without the presence of matter. And also this wave normally travels through space in a straight line, and will vary only slightly in different atmospheric and weather conditions. Because of this, satellites can use radars to work on projects outside of the Earth's atmosphere and on other planets. Electromagentic waves travel at a constant speed through a vacuum called the speed of light abbreviated by the letter "C" (3×10^8 meters per second). This is very useful to know to when doing ranging calculations. So the slant range which is the actual distance from the radar to the target can be determined by the Formula 2.1.

$$R = C \cdot t/2 \qquad \text{(Eq2.1)}$$

Where R is the slant range, C is the speed of light ($3\times 10^8 \mathrm{m/s}$), t is the time delay between transmitted signal and returned signal. Since the signal hits the target and then returns, the time is the round trip time which should be divided by 2 to get one way trip time.

2.2 Radar Types and Applications

Radar was originally devised as an instrument to detect approaching ships or aircraft

in military purpose. Practice and experience in reading the scope soon showed that radar could do much more. Nowadays, the radar has been used in civil applications, including navigation of ships, aircraft and spacecraft, remote sensing of the environment, and law enforcement.

For different kinds of radar application, the important parameters (ranges, sizes, shapes, velocity, etc) of target to be detected may vary. Different radar types were developed for different detection missions.

- Simple Pulsed Radar: This is a very simple type of radar that is used in ground penetrating radar and imaging radars. In this system, the transmitter transmits short pulses of radio or microwave signals. This is useful radar for finding objects.
- Continuous Wave Radar: This type of radar system transmits a continuous wave rather than short pulses and analyzes the change in frequency of the returned signal. This is a good type of radar to determine the velocity of objects.
- Synthetic Aperture Radar (SAR): To increase the resolution of a radar image, a very large antenna with a narrow beam width is necessary. Since very large antennas can sometimes be impractical, synthetic aperture radar was developed to use a small radar antenna like it was a large one. To accomplish this SAR repeatedly takes measurements from several positions. These measurements are then processed like they were taken from a single large antenna.
- Phased Array Radar: This radar uses many very small antennas that can be rotated to comprise a very large antenna that can change its beam direction very quickly.
- Secondary Radar: This kind of radar uses coded signals to be transmitted and

received to allow communication between targets. This type of radar is used in air traffic control.

2.3 Doppler Radar Basics

2.4.1 Doppler Effect

The Doppler effect is the effect that is produced by a moving source of waves in which there is an obvious shift upward in the frequency for people or observers towards whom the source is approaching and an obvious shift downwards in the frequency for people from whom the source is moving away. This shift in effect does not occur because of the real change in frequency of the source. The effect only changes because of the change in distance. The Doppler effect can be observed in any type of wave whether water wave, sound wave, or light wave.

One perfect example of the Doppler effect will be an ambulance or a fire engine truck running on a highway with its siren blaring. While the vehicle was traveling towards you, you could hear the high pitch of the siren, but suddenly after you pass it by the pitch lowers and drops. The very obvious shift in frequency of a sound wave will be produced by a source on the move.

2.4.2 Doppler Radar

Doppler radar is a kind of radar which uses the Doppler effect to measure the radial velocity of targets in the antenna's directional beam. In Doppler radars the signal is sent out a constant rate. This signal is then shifted according to the Doppler effect as it returns. The amount of the signal shift depends up on the speed of the target. This signal is picked up and interpreted with greater accuracy that the other radars.

Either one or both of the objects may be moving with respect to the ground. When the two objects are approaching each other, the Doppler shift causes a shortening of wavelength or increase in frequency. When the two objects are receding from each other, the Doppler shift causes a lengthening of wavelength or decrease in frequency.

For a Doppler radar system to measure speed, an accurate sample of the original phase of the transmitted signal must be maintained for comparison against the reflected signal. Radar Doppler shift frequency (f(t)) is a function of radar transmit frequency (f_o), speed of wave (c = speed of light), and target velocity (Vt). Note, Vt is positive (+) for approaching targets and negative (-) for receding targets. This effect occurs twice, on the radar-target and target-radar paths: the total Doppler shift is then:

$$f(t) = \pm\frac{2V_t f_o}{c} = \pm\frac{2V_t}{\lambda} \qquad \text{(Eq 2.2)}$$

When the target undergoes a periodic movement x(t) with no net velocity, the Doppler shift of the reflected signal can be better described as a phase modulation.

$$\theta(t) = \frac{2f}{c}\big(2\pi x(t)\big) = \frac{4\pi x(t)}{\lambda} \qquad \text{(Eq 2.3)}$$

When a person’s chest is the target, as shown in Figure 2.1, the phase is modulated in direct proportion to the chest displacement. When the phase is demodulated, the resulting

signal is proportional to the time-varying chest position, from which the heart and respiration rates can be determined.

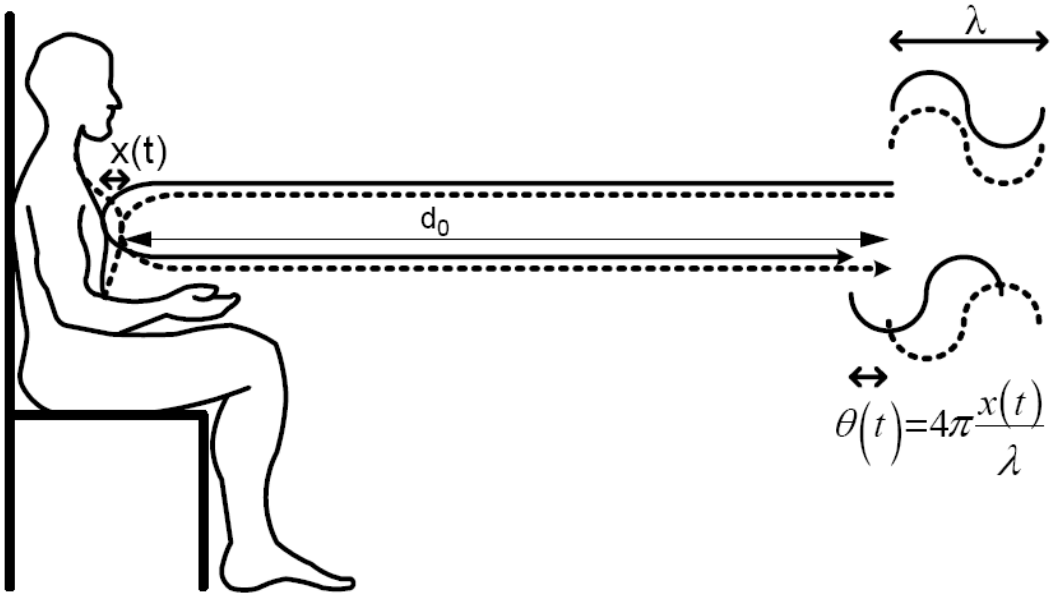

Figure 2.1 Cardiopulmonary monitoring with Doppler radar

The Doppler radar has been used for physiological motion monitoring since 1970's. Both contact and non-contact techniques have been shown effective for detection of pressure pulse, and cardio-pulmonary activity. Possible applications include medical monitoring, sense-through-the wall military applications, search and rescue applications, and driver's status monitoring.

CHAPTER 3

IQ DEMODULATOR AND SIGNAL PROCESSING

3.1 Doppler Transceiver System

Doppler radar physiological monitoring has been known since 1970's. A number of similar custom transceivers were developed, including a life detection system operating at a distance of up to thirty meters, and a superficial temporal artery monitor for military pilots. The use of CW, FM, and UWB radar has been explored for physiological sensing. Doppler radar transceiver implementations range from using laboratory equipment, to integration on a printed circuit board, and on a single silicon chip. Single channel and quadrature radar has been used, and linear and non-linear demodulation methods have been proposed.

By the Doppler effect, an RF wave reflected at a moving surface undergoes a frequency shift proportional to the surface velocity. If the surface is moving periodically, such as the chest of person breathing, this can be characterized as a phase shift proportional to the surface displacement. If the movement is small compared to the wavelength, a circuit that couples both the transmitted and reflected waves to a mixer can produce an output signal with a low-frequency component that is directly proportional to the movement. The mathematics analysis for the signal channel transceiver and quadrature channel transceiver will be introduced in the following sections. The

quadrature system is used to overcome the limitations of signal channel transceiver.

3.1.1 Single Channel Transceiver

The Figure 3.1 shows a simple Doppler transceiver system, which contains transmit and receive antennas, signal source, splitter, mixer and a low pass filter.

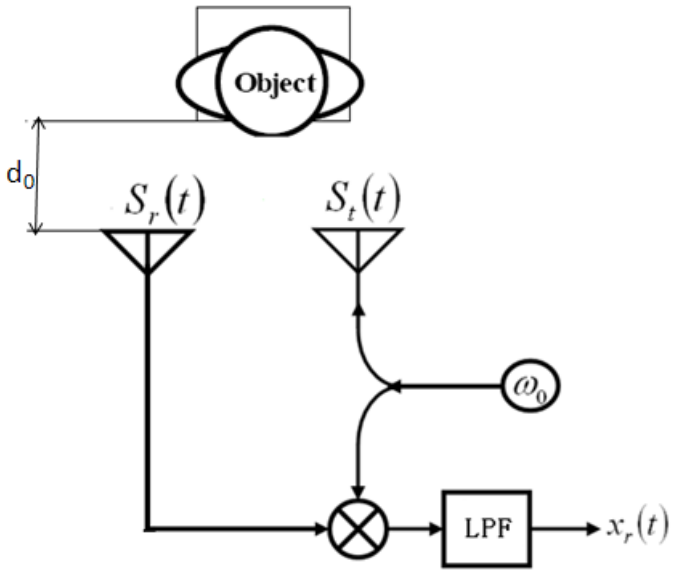

Figure 3.1 Simple Doppler transceiver system

According to the Doppler radar theory, the phase shift between the transmitted signal and received signal can tell the velocity of the target. To compare the phases of two signals:

$$S_r(t)S_t(t) = A\cos\left[\omega_0 t + \frac{2\pi}{\lambda}(2d_0 + 2d(t))\right]\cos(\omega_0 t) \qquad \text{(Eq 3.1)}$$

Apply trigonometric identities, to Eq 3.1,

$$S_r(t)S_t(t) = \frac{A}{2}\cos\left[\frac{2\pi}{\lambda}(2d_0 + 2d(t))\right] + \frac{A}{2}\cos\left[2\omega_0 t + \frac{2\pi}{\lambda}(2d_0 + 2d(t))\right] \qquad \text{(Eq 3.2)}$$

The second term of Eq 3.2 is twice frequency as the transmitted signal which will be filtered out by the low pass filter. After that,

$$X_r(t) = \frac{A}{2}\cos\left[\frac{2\pi}{\lambda}\left(2d_0 + 2d(t)\right)\right] \quad , \qquad \text{(Eq 3.3)}$$

Which has a variable phase,

$$\varphi(t) = \frac{2\pi}{\lambda}2d(t) \qquad \text{(Eq 3.4)}$$

This is the phase change which is detected by the radar upon the movement of the target. In fact, this single channel receiver is very simple and is capable of producing a baseband signal with sufficient accuracy for extracting vital signal. But there is a problem with it as null and optimum location of the subject under test.

The null case happens when the distance of the subject to the radar is an integer multiple of quarter of wavelength:

$$d_0 = \frac{n}{4}\lambda \qquad \text{(Eq 3.5)}$$

In this case, the Eq 3.4 is transformed after mathematical analysis:

$$X_r(t) \approx \pm\frac{A}{2} \qquad \text{(Eq 3.6)}$$

In the null case, the receive signal is almost a constant which does not provide much useful information about the target.

The optimum case will happen when the distance between the subject and the radar is an odd multiple of eighth of wavelength.

$$d_0 = \frac{2n+1}{8}\lambda \qquad \text{(Eq3.7)}$$

In this case, the Eq 3.5 is transformed after mathematical analysis:

$$X_r(t) \approx \pm\frac{A}{2}\varphi(t) \qquad \text{(Eq 3.8)}$$

In the optimum case, the received signal will most closely follow the motion of the target. The distance between the optimum point and the null point is λ/8.

3.1.2 Quadrature System

In order to avoid the null case in the single channel transceiver system, a quadrature system with two receive channels (in-phase and quadrature) is depicted in Figure 3.2. The quadrature system is made of transmit and receive antennas, two mixers, 90 degree splitters. The LO signal is split to feed the two mixers. For the Q channel, it goes through a 90 degree phase shifter and then is mixed with the received signal to generate

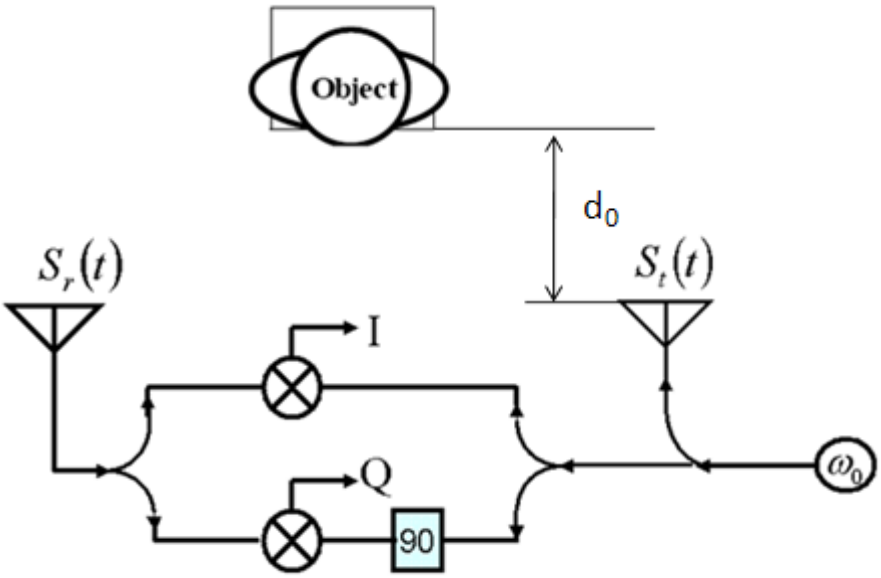

Figure 3.2 Quadrature system

the quadrature channel output. For the I channel, the output is

$$X_{rI}(t) = \frac{A}{2}\cos\left[\frac{2\pi}{\lambda}\left(2d_0 + 2d(t)\right)\right] \qquad \text{(Eq 3.9)}$$

For the Q channel,

$$X_{rQ}(t) = \frac{A}{2}\cos\left[\frac{2\pi}{\lambda}\left(2d_0 + 2d(t) - \frac{\pi}{2}\right)\right] = \frac{A}{2}\sin\left[\frac{2\pi}{\lambda}\left(2d_0 + 2d(t)\right)\right] \qquad \text{(Eq 3.10)}$$

Because of the two channel outputs, if the subject is in the null point for one of the channels, for the other channel the subject will be in the optimum point. The quadrature system overcomes the limitation of the single channel system. However, quadrature

system is more complex: the RF hardware includes two receiver chains that must be balanced, and a reliable method to combine the I and Q baseband information is required to enable accurate phase detection.

3.2 Signal processing

A Doppler radar for physiological motion sensing, transmits a radio wave signal and receives a motion-modulated signal reflected from a target. The RF wave reflected at a moving surface undergoes a phase shift proportional to the surface displacement. Assuming the target's time varying displacement is $\Delta x(t)$, the baseband amplitude due to receiver and mixer gain is A_r. The baseband output signal for I and Q channel can be expressed as:

$$B_I = A_r \cos\left(\theta + \frac{4\pi\Delta x(t)}{\lambda}\right) \qquad \text{(Eq 3.11)}$$

$$B_Q = A_r \sin\left(\theta + \frac{4\pi\Delta x(t)}{\lambda}\right) \qquad \text{(Eq 3.12)}$$

Where θ is the constant phase shift related to the phase change at the surface of a target and the phase delay between the mixer and antenna.

Applying arctangent demodulation to the ratio of the quadrature outputs, phase information linearly proportional to target's motion can be extracted as:

$$\emptyset(t) = \arctan\left(\frac{B_Q(t)}{B_I(t)}\right) = \arctan\left(\frac{A_r \sin\big(\theta + p(t)\big)}{A_r \cos\big(\theta + p(t)\big)}\right) = \theta + p(t) \qquad \text{(Eq 3.13)}$$

$$p(t) = \frac{4\pi\Delta x(t)}{\lambda} \qquad \text{(Eq 3.14)}$$

The figure 3.3 shows the complex plot of quadrature outputs due to the target's periodic

motion Δp(t). VI and VQ are the DC offset at I and Q channel respectively. Ar is proportional to the received signal power.

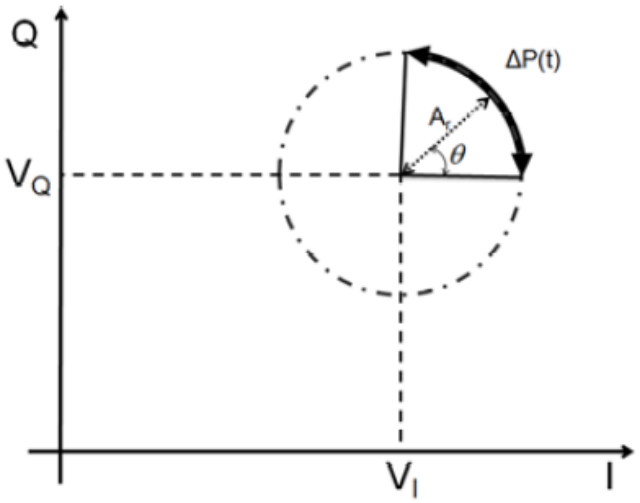

Figure 3.3 Complex plot of quadrature outputs

To do arctangent demodulation (non-linear), the data is first multiplied by the transpose of the matrix of eigenvectors of the covariance matrix to rotate the arc. Thereby the dc offset becomes an offset purely on the I-axis. Since after rotation, the Q-component is always in an optimum point (and the I-component always in a null point), we can simply use the Q-component as the demodulated signal. If the arc length is relatively small, it can be approximated with a line, resulting in a linear demodulation method which is a method of transposing multi-dimensional data to a single dimension, suppressing redundant information and maximizing the variance in the data. Because all the DC information was removed in the linear demodulation, the output can only be proportional to the received signal power. But the non-linear demodulated signal contains dc information which enables the output to present absolute displacement of moving target.

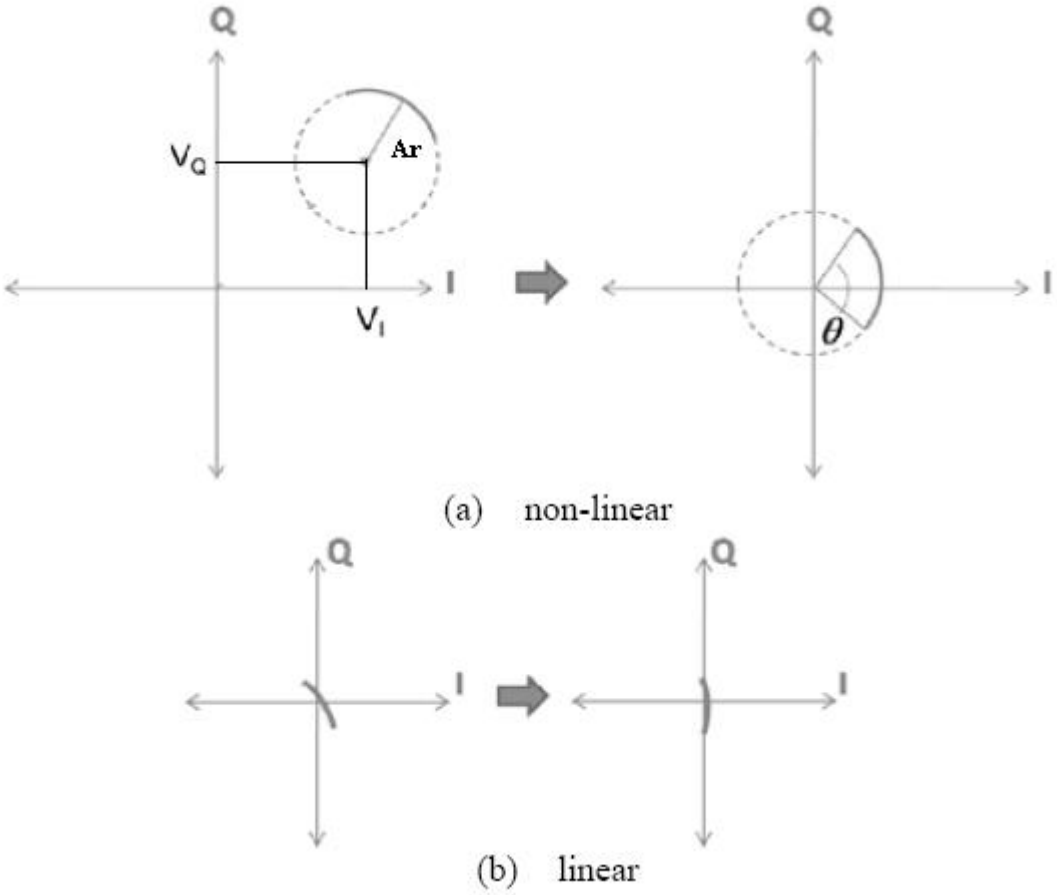

Figure 3.4 Non-linear and linear demodulation

If analog high-pass filters are used to eliminate the dc components of the signal, the filter phase delay will cause signal distortion for all components below or close to the cut-off frequency, resulting in less measurement accuracy.

3.3 Printed Circuit Board Design Needs of I/Q Demodulator

The quadrature receiver is also referred to as a quadrature detector, or I/Q demodulator. The components of the I/Q demodulator include two mixers, one zero degree power splitter which splits the RF input signal equally without any phase change to feed the RF ports of the two mixers, and one 90 degree power splitter which splits the LO input signal equally with a 90 degree phase shift to feed the LO ports of the mixers.

The diagram of the I/Q demodulator is depicted in Figure 3.5.

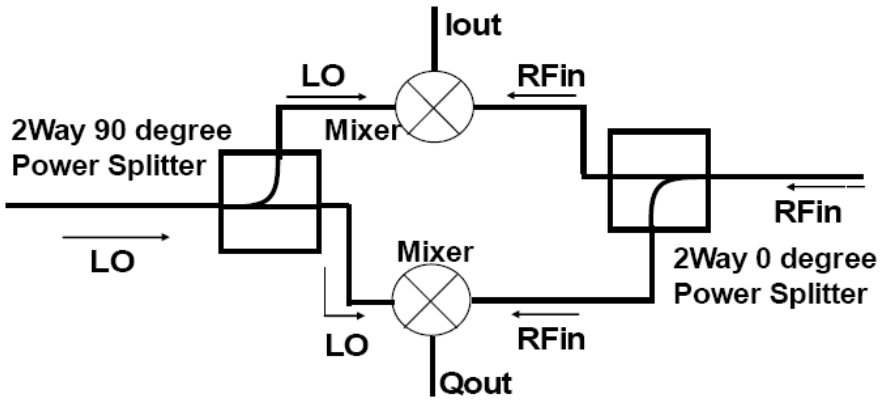

Figure 3.5 IQ demodulator diagram

3.3.1 Goals for Power Divider

On the PCB, an RF signal splitter, a precision quadrature LO signal splitter and two high linearity downconverting mixers are integrated. The chips directly downconvert an RF signal to baseband, and demodulate the in-phase (I) and quadrature (Q) signal components.

In order to make the I and Q channel balanced, the design of the RF signal splitter and quadrature LO signal splitter is very important. The function of the RF signal splitter should ensure the RF input signal split equally without any phase shift. The function of the quadrature LO signal splitter should ensure the LO input signal split equally but with a 90 degree phase shift. The devices' matched I and Q channels ensure precise gain and phase matching, so that significantly less calibration is required.

3.3.2 Goals for I/Q Mixer

The mixer on board need to have high linearity, and high LO to RF isolation. The nonlinearity of the mixer can cause interference with the desired signal which affects the accuracy of radar detection. A balanced structure has high LO to RF isolation, which suppresses both the down-conversion of LO amplitude noise and self-mixing, which leads to a dc current that causes 1/f noise generation. Baseband 1/f noise created by the mixer can be a dominant noise source for Doppler radar. Use of a passive mixer minimizes 1/f noise, which is caused by fluctuations in the channel resistance of CMOS devices. Isolation between the LO and the RF input signals is important also because leakage between the LO and the RF ports in a direct-conversion receiver can lead to large dc offsets.

CHAPTER 4

IQ DEMODULATOR DESIGN

4.1 Power Divider Design

4.1.1 Power Dividers and Directional Couplers Properties

Power divider and directional coupler are passive microwave component used for power division and power combining. The figure 4.1 shows the three-port network. In power division, an input signal is divided by the coupler into two (or more) signals of lesser power. In power combining, two (or more) signals are combined into an output signal.

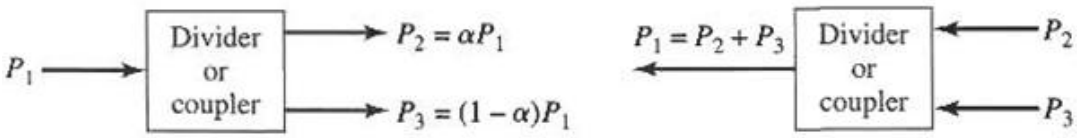

Figure 4.1 (left) power dividing; (right) power combining

Power dividers are often of the equal-division (3 dB) type, but unequal power division ratios are also possible. A directional coupler couples part of the transmission power by a known amount out through another port, often by using two transmission lines set close enough together such that energy passing through one is coupled to the other.

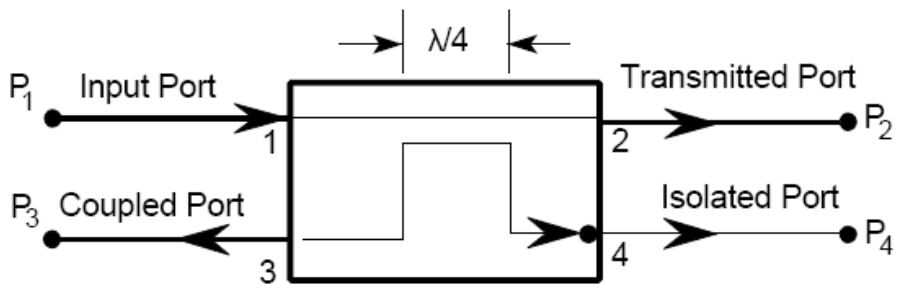

Figure 4.2 Diretional coupler

As shown in Figure 4.2, the device has four ports: input, transmitted, coupled, and isolated. The term "main line" refers to the section between ports 1 and 2. Often the isolated port is terminated with an internal or external matched load (typically 50 ohms). Common properties desired for all directional couplers are wide operational bandwidth, high directivity, and a good impedance match at all ports when the other ports are terminated in matched loads. These performance characteristics of hybrid or non-hybrid directional couplers are self-explanatory.

4.1.2 Branch-line Coupler Design

4.1.2.1 Geometry of Branch-line coupler

The branch-line coupler is the simplest type of quadrature coupler, since the circuitry is entirely planar. Generally branch-line couplers are 3dB, four ports directional couplers having 90 degree phase difference between its two output ports named through and coupled arms. The branch-line coupler can be made in two forms: microstrip line and

stripline. The following figure shows the geometry. The left picture in Figure 4.3 shows the geometry of microstrip line used in branch-line coupler. The right picture shows the geometry of stripline used in branch-line coupler.

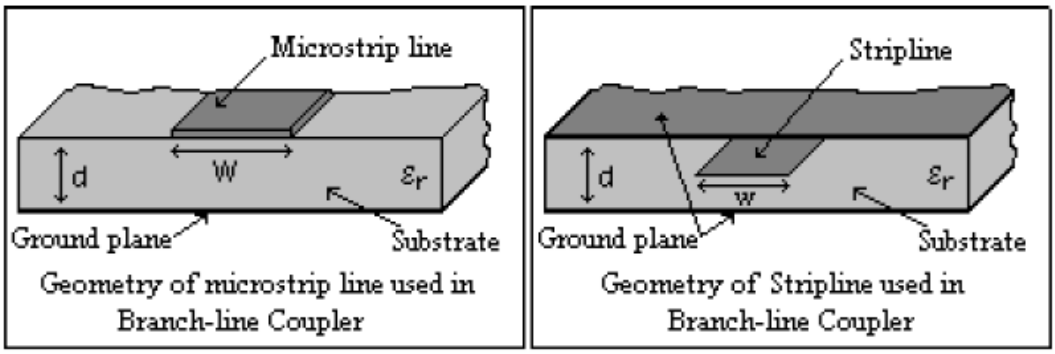

Figure 4.3 Geometry of microstrip line used in branch-line coupler(left); Geometry of stripline used in branchline coupler (right)

The branchline coupler, which will be designed in this section, is made in mircrostrip and will work at 2.4 GHz as its center frequency. An ideal branch-line coupler (Figure 4.4) is made of two main transmission lines shunt-connected by two secondary (branch lines). The first port is the input port, and the signal is split into two quadrature signal on the port 2 andport 3. The port 4 is isolated from the input port at the center frequency.

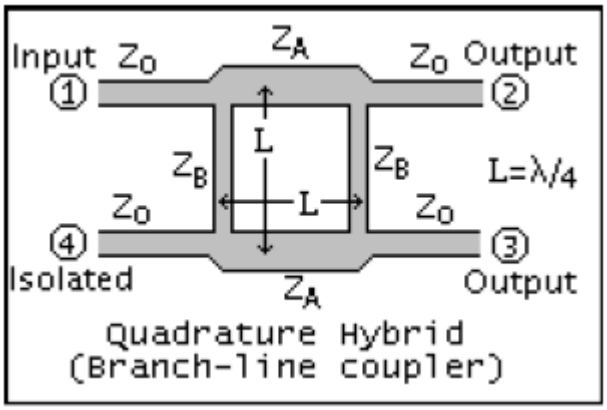

Figure 4.4 Ideal branch-line coupler

The length (L) of the branch line and series line is one fourth of the design wavelength. Then L can be found as following.

$$L = \lambda/4, \quad \lambda = v_p/f = c/f\sqrt{E_r} \quad \Rightarrow \quad L = c/4f\sqrt{E_r} \qquad \text{（Eq 4.1）}$$

For the design purposes, the center frequency of the branch-line coupler is 2.4GHz. The dielectric constant of the substrate (R3003) is 3.0. When the f = 2.4GHz, Er = 3.0, and c = 3×10^8 m/s, the L will be 18mm from the Eq 4.1. For the ideal branch-line coupler, the length of the four arms is same. The width of each arms will be calculated in following section depended on the impedance choices.

According to the impedance choice of the series and stub microstrip transmission lines we can calculate the w/d ratios of those lines in microstrip form by using the following formulas:

$$\frac{W}{d} = \begin{cases} \dfrac{8e^{A}}{e^{2A}-2} & \text{for} W/d < 2 \\ \dfrac{2}{\pi}\left[B - 1 - \ln(2B-1) + \dfrac{E_r - 1}{2E_r}\left\{\ln(B-1) + 0.39 - \dfrac{0.61}{E_r}\right\}\right] & \text{for } W/d > 2 \end{cases}$$

$$A = \frac{Z_0}{60}\sqrt{\frac{E_r+1}{2}} + \frac{E_r - 1}{E_r + 1}\left(0.23 + \frac{0.11}{E_r}\right)$$

$$B = \frac{377\pi}{2Z_0\sqrt{E_r}}$$

(Eq 4.2)

For the series transmission line, impedance Zo is 35.35 ohm, and dielectric constant Er of the substrate is 3.0, so A and B could be calculated. As a result, A is 0.966, B is 9.667. Once we got the value for A and B, the W/d ratio could be gotten. If W/d is smaller than 2, W/d equals to 4.3 which againsts the assuming condition. If W/d is larger than 2, W/d equals to 4.165 which fits the assuming condition and this value will be taken. The thickness of the substrate material (R3003) is 0.25mm which is also the d value in the

formula, so the width of the series transmission line is 1.041mm.

For the stub transmission line on the same substrate, impedance Zo is 50ohm, Er is 3.0. A and B can be calculated as 1.312 and 6.8 respectively. W/d is 2.52 by calculated under the ratio is smaller than 2 condition, which is not reasonable. In the other condition, the W/d is 2.49, which is larger than 2. The thickness is 0.25mm, so the width of the stub transmission line is 0.622mm.

Once the dimensions of the transmission lines have been gotten theoretically, the schematic of my design could be drawn following the Figure 4.5 in Agilent ADS.

4.1.2.2 Simulation and Layout for Branch-line Coupler

The Figure 4.5 is the schematics of the proto-design in ADS. The length of the four transmission line is 18mm, and the width of the series transmission is 1.401mm, and the width of the stub transmission line is 0.622mm. All the parameters are calculated by theory.

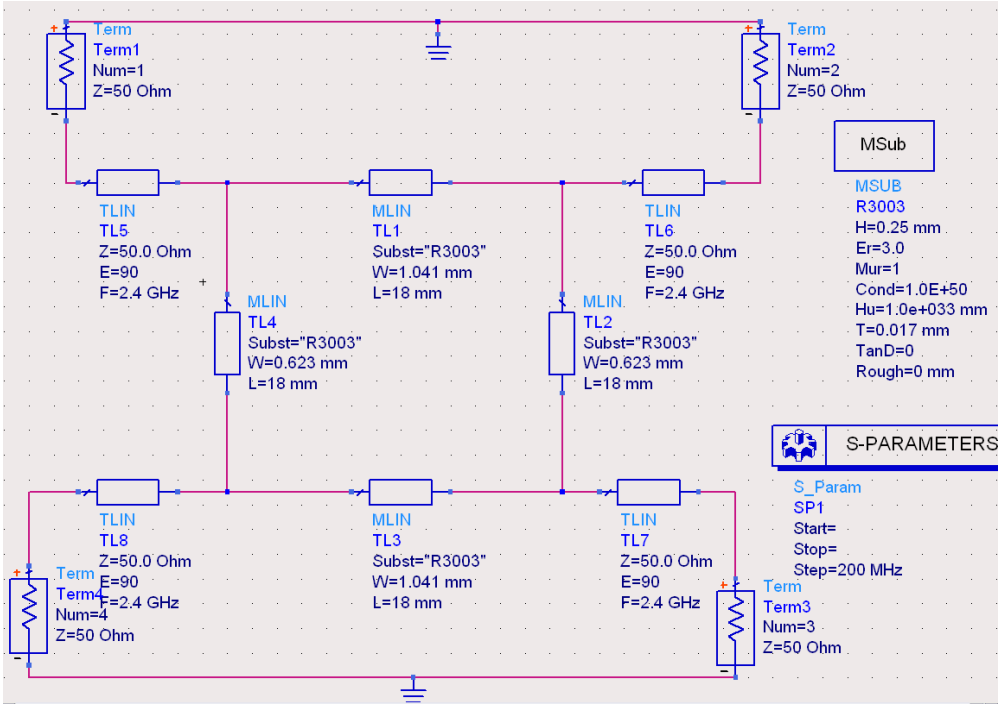

Figure 4.5 Schematic of Branch-line Coupler

The schematic is built on the R3003 substrate, simulated from 1.4 GHz to 3.4 GHz step by 0.2GHz. Combine with the theoretical calculation and simulation results, when the L is 20 mm. The performance achieved the expectation. Figure 4.6 is the transmission loss from port 2 to port 1, and from port 3 to port 1. Using the ideal transmission line impedances shown above provides an equal 3 dB split at the center frequency.

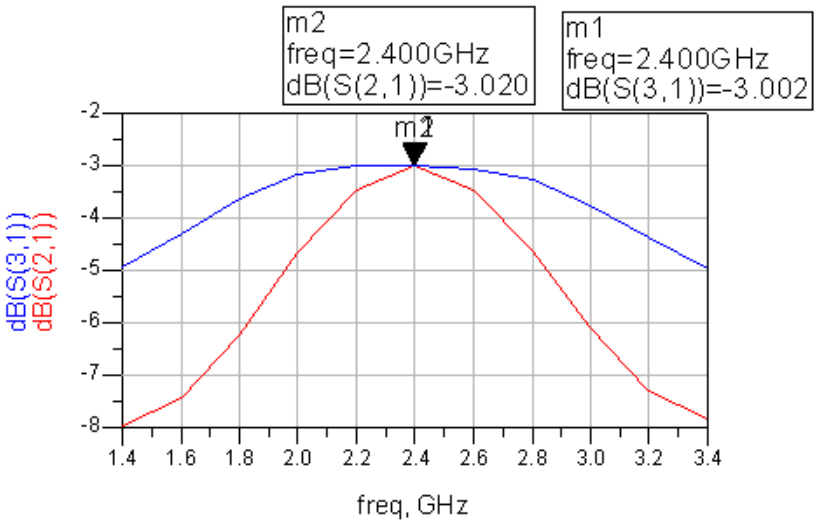

Figure 4.6 Transmission Loss

The return loss is minimum (-40dB) at the center frequency. The isolation between port 2

and port 3 is nearly equal to the return loss.

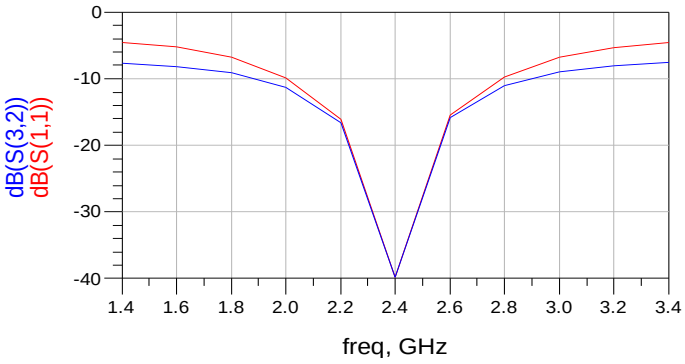

Figure 4.7 Return Loss (red) and Isolation (blue)

The main feature of the Brach-line coupler is the 90 degree phase difference between the two outputs (port 2 and port 3). The Figure 4.8 is the phase change of the outputs. The marker 3 and marker 4 tell the phase at the center frequency for port 3 and port 2 separately. As we can see the phase difference is 179 degrees minus 89 degrees which is 90 degree. That is exactly the phase change required in this design.

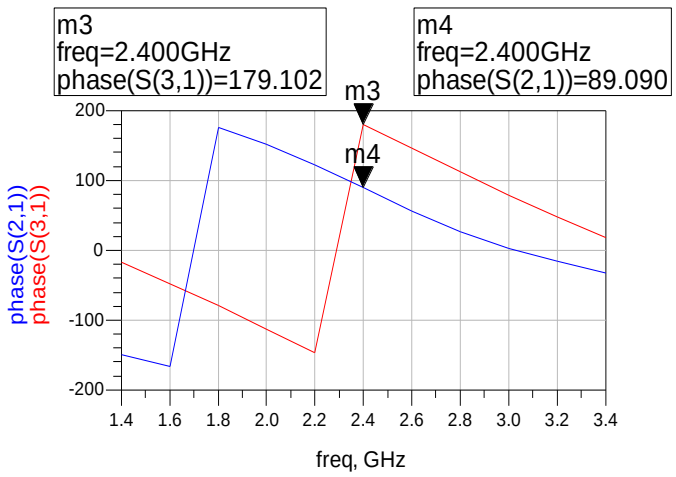

Figure 4.8 Phase Response

The layout was drawn as shown Figure 4.9. The width for the series transmission line is 1.041mm; the length for the series transmission line is 20mm. And the width for the

stub transmission line is 0.623mm; the length for the stub transmission line is 20mm as well. The layout is built on R3003 substrate, and simulated in the same environment. The simulation results for the layout match the simulation results for the schematic.

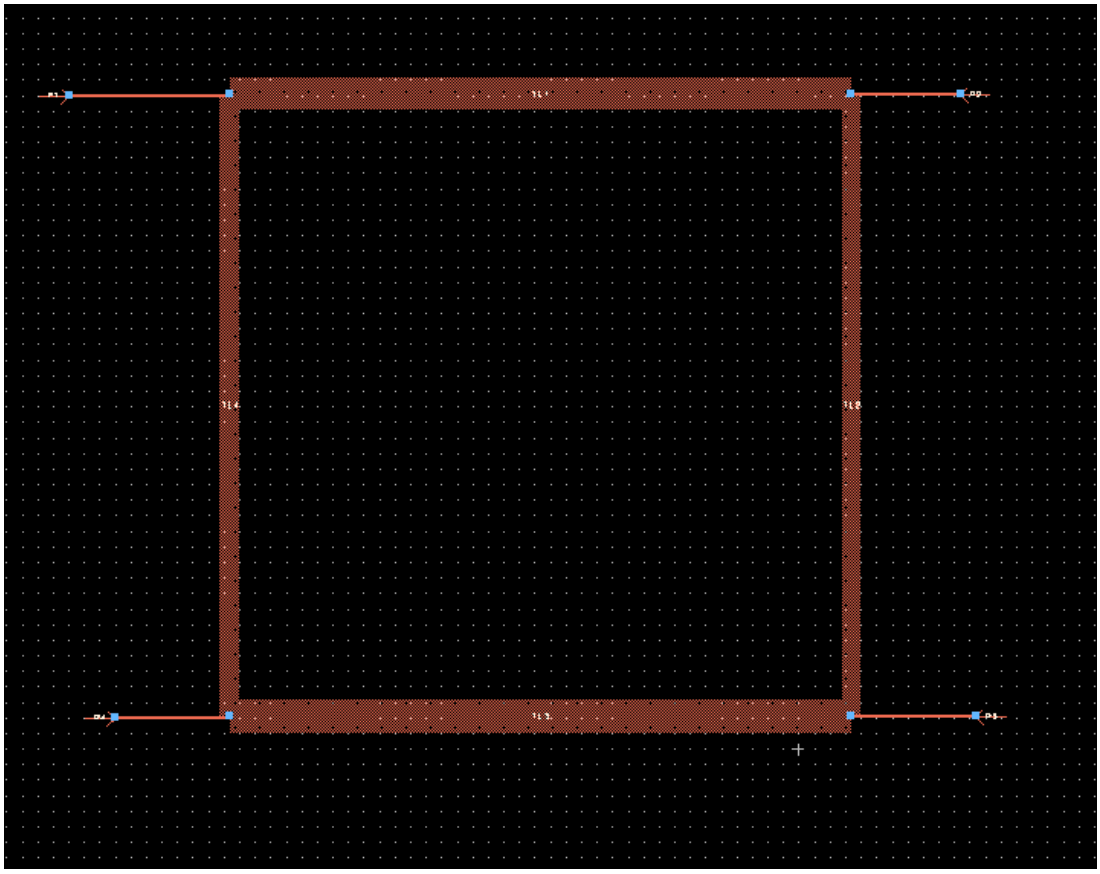

Figure 4.9 Layout of Branch-line Coupler

4.1.3 Wilkinson power divider design

4.1.3.1 Geometry of 3-port Wilkinson Power Divider

The Wilkinson power divider was invented around 1960 by Ernest Wilkinson. It splits an input signal into two equal phase output signals, or combines two equal-phase signals into one in the opposite direction. Wilkinson relied on quarter-wave transformers to match the splitter ports to the common port. And it’s impossible for a three-port network to be

reciprocal, lossless and matched all at the same time. You can only have 2 of these properties. So a 50 ohm resistor is added as the isolation resistor in a Wilkinson power splitter. The resistor does not only allow all three ports to be matched, it fully isolates port 2 and port 3 at the center frequency. The resistor adds no resistive loss to the power split, so an ideal Wilkinson splitter is 100% efficient.

Figure 4.10 shows the layout of a classical microstrip Wilkinson power splitter. In the simplest form, it consists of two quarter-wave line segments at the center frequency $f_{o,}$ with characteristic impedance Z_o $\sqrt{2}$, and a 2 Z_o lumped resistor connected between the output ports. It provides low loss, equal split, matching at all ports, and high isolation between output ports.

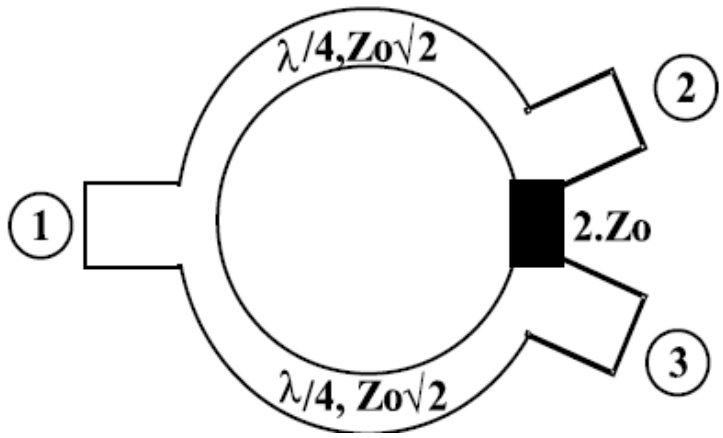

Figure 4.10 Classical Mircostrip Wilkinson Power Divider

For the design purposes, the center frequency of the Wilkinson power divider is 2.4GHz. The length of the quarter-wave line is 18mm, same as for branch-line coupler, which helps to get the radius of the transmission ring of 5.7mm. Using the same formula (Eq 4.2) to calculate the w/d ratios, when the impendance Z_o is 70.7 ohm, E_r is 3, assuming w/d ratio is greater than 2, the ratio calculated is 1.2 which conflicts with the assumption. If the w/d ratio is smaller than 2, the ratio calculated is 1.4 which is

reasonable. The d is 0.25mm which is the thickness of the substrate, so the width of the microstrip line is 0.35mm.

4.1.3.2 Simulation and Layout for Wilkinson Power Divider

After the calculation process for the parameters of the transmission lines in the Wilkinson power divider, the schematics is built in Agilent ADS which follows the layout of the classic Wilkinson power divider. There are two semi-circle transmission curves to build the transmission ring part. The width is 0.35mm according to the theoretical calculation, and the radius is 6.5mm to achieve best simulation results.

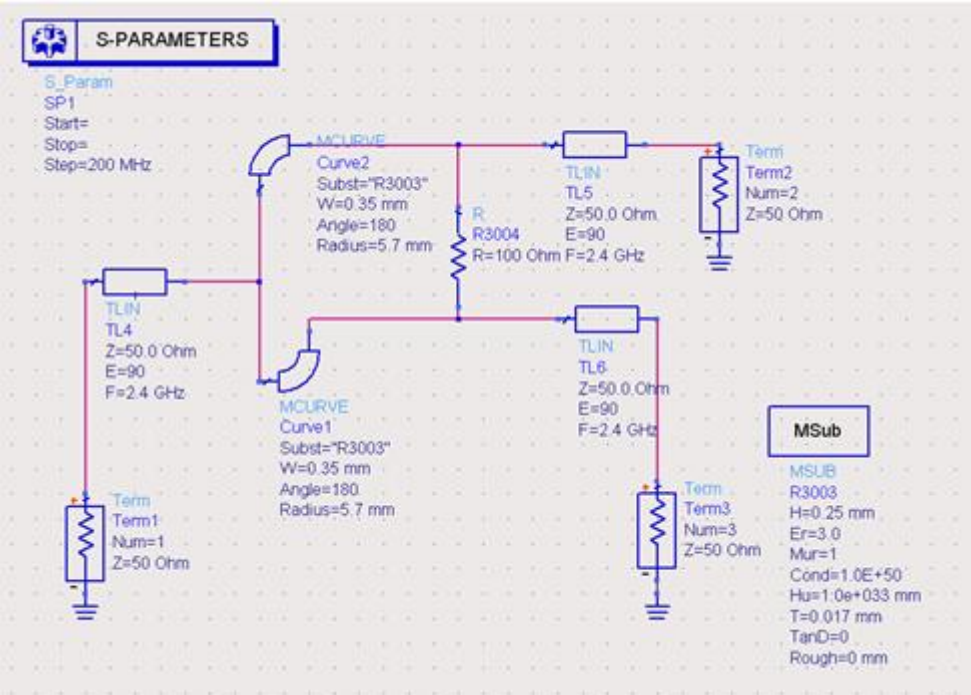

Figure 4.11 Schematics of Wilkinson power divider

The schematics is built on the R3003 substrate, and simulated from 1.4 GHz to 3.4 GHz step by 0.2 GHz. The Figure 4.12 shows the loss from input (port 1) to outputs (port 2 and port 3). The equal 3 dB split is provided at the center frequency.

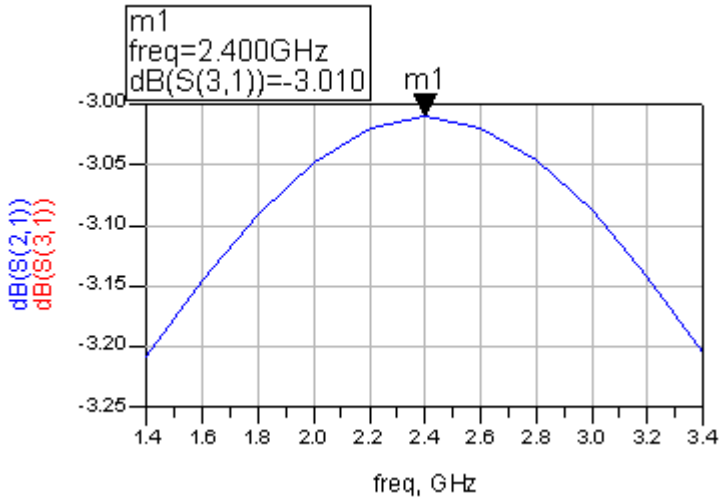

Figure 4.12 Transmission Loss

The Figure 4.13 shows the return loss and isolation. The return loss is the power reflected at input (port 1). The minmum return loss is -55 dB at the center frenqucy. The isolation is nearly equal to the return loss. Both of return loss and isolation reach their minmum value at the center frequency.

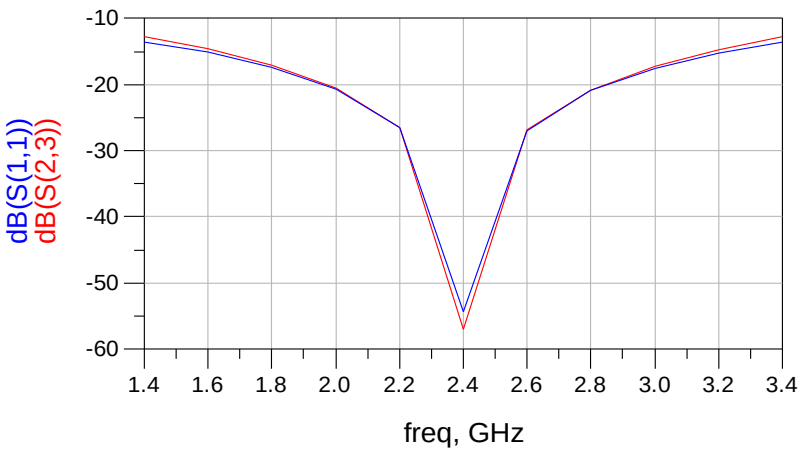

Figure 4.13: Return Loss (blue) and Isolation (red)Figure 1

The layout is made of two 180 degree transmission curves, a resistor pad, and a short transmission line, and build on R3003 as substrate. The width of the transmission curve is 0.35mm, and the radius is 6.5mm. The resistor pad consists of two conductive metal pads

which are used to solder a rectangular chip resistor. The short transmission line is 0.62 in width and 1 mm in length which provide 50 ohm impendance between the two transmission line curves.

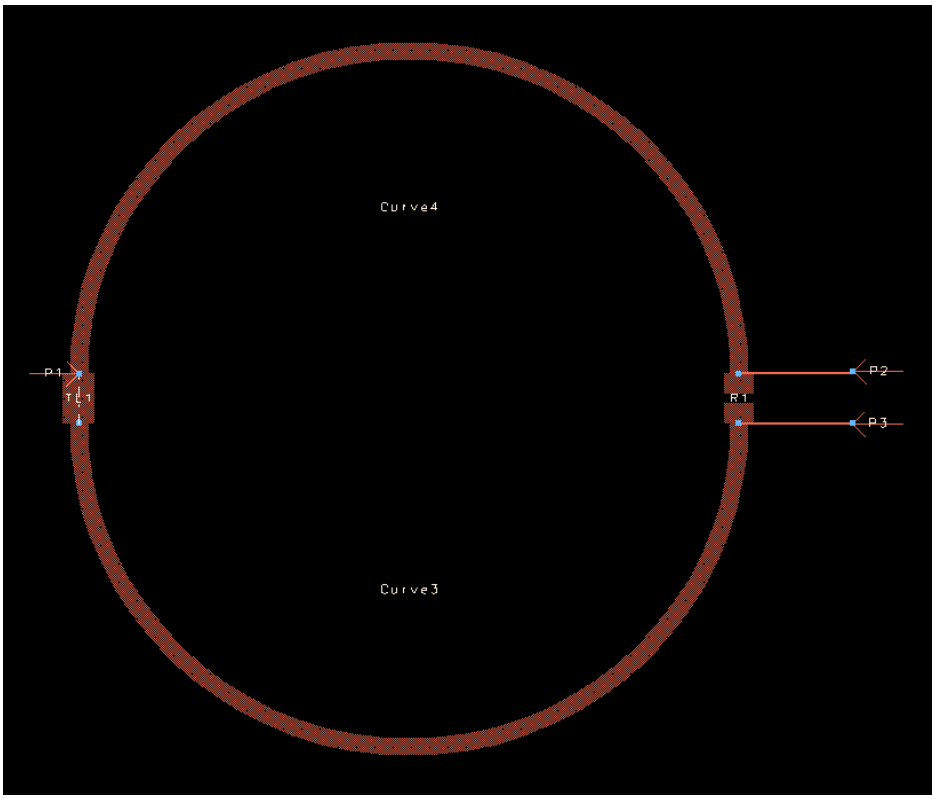

Figure 4.14 Layout of Wilkinson Power Divider

4.2 Passive Mixer on PCB

The mixer, which will be used in the I/Q demodulator, is a 2.4GHz resistive ring mixer with on-chip baluns. They are fully integrated on chip in 0.18um IBM7HP process. This is the first reported double-balanced passive mixer with integrated RF and LO baluns.

The schematic of this mixer circuit is shown in Figure 4.15. This mixer circuit

integrates 3 parts: RF balun (Fig 4.15(a)), mixer core (Fig 4.15(b)), and LO balun (Fig.4.15(c)). The four FET ring mixer which is a well know double-balanced resistive mixer, which provides a double balanced solution with high linearity and good port to port isolation.

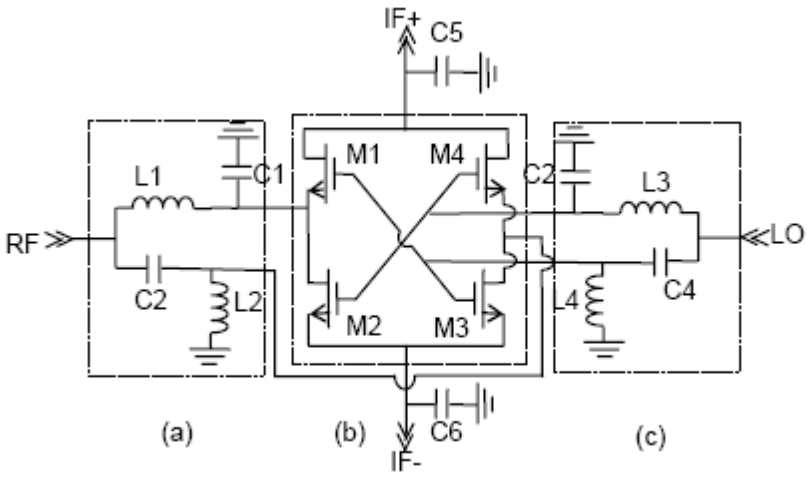

Figure 4.15 Schematic of the mixer with baluns. (a) RF balun; (b) NMOS ring mixer; (c) LO balun

The mixer die is tested on the Cascade probe station. This mixer exhibits broadband RF impedance matching with return loss better than -10 dB through the RF frequency range from 2 to 6 GHz. The conversion loss of 7.8 dB is achieved at the RF frequency 2.4 GHz. This mixer provides 6 dBm of the input P1dB, and 13.4 dBm of the input IP3 at the operating RF frequency. The LO-RF isolation of -52.7dB and the LO-IF isolation of -30 dB are achieved at 2.4GHz.

In order to mount the mixer in the PCB, it is packaged in QFN01603 by the Kansas City Plant (KCP) using 7HP technology. The QFN01603 is a small outline-surface mount package made by SPECTRUM, semiconductor material incorporation. The bounding diagram of the mixer die is shown in Figure 4.16. The interconnection of the mixer can’t

be seen on the die, but the labels of each pad tell the outside connection with the inside circuit. The pad on the upper left corner will be wired to the first pin on the left side of the package which is also the pin 1 for this package.

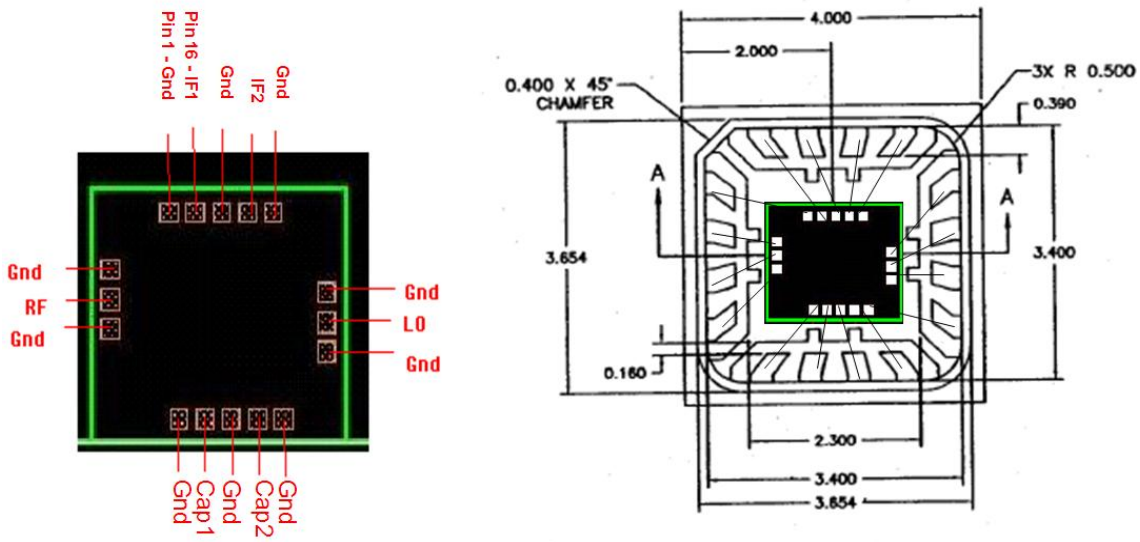

Figure 4.16 Mixer Bonding Diagram

The printed circuit board is drawled based on the bottom view of the package. The copper (red) is the conduct material which provides the connection for the pins of the package and the board. The holes (blue) on the center pad are the plated through-holes which provide ground connection through ground plane to the top layer. The center pad is 2.3 mm by 2.3 mm, the size of the pins are 0.3 mm by 0.4 mm.

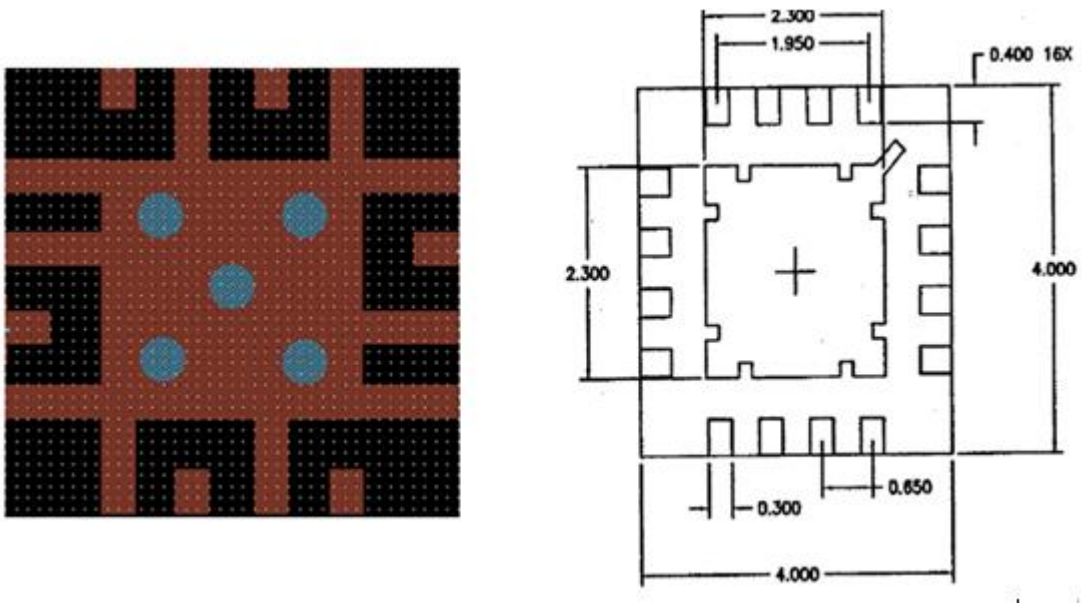

Figure 4.17: PCB for Mixer: PCB layout (left); Package Bottom View (right)

4.3 PCB of IQ Demodulator

4.3.1 PCB

Since the designs of power dividers were made, now the IQ demodulator is generated by integrate the layout of power dividers and PCB for mixer together.

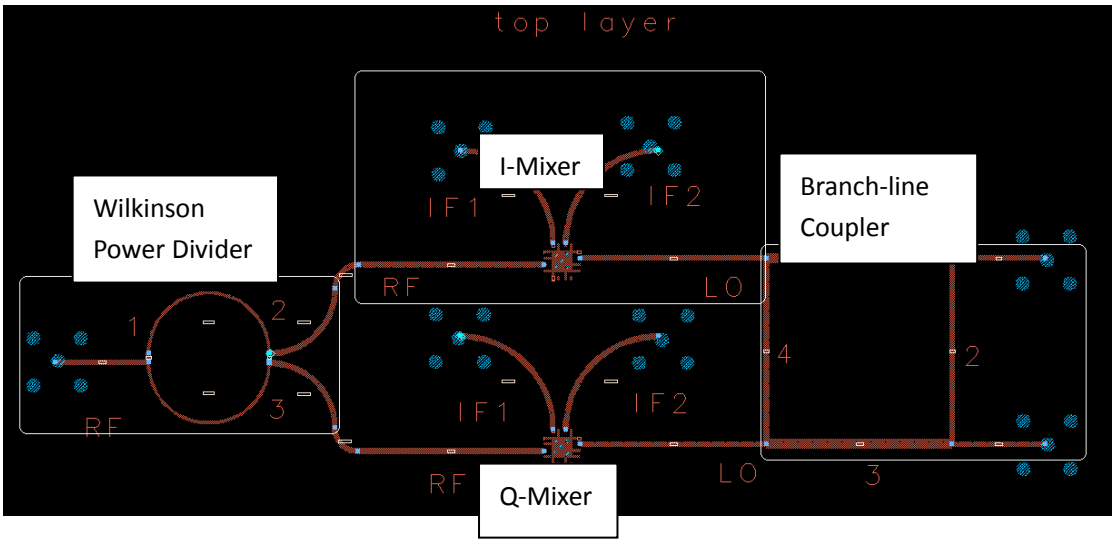

(a)

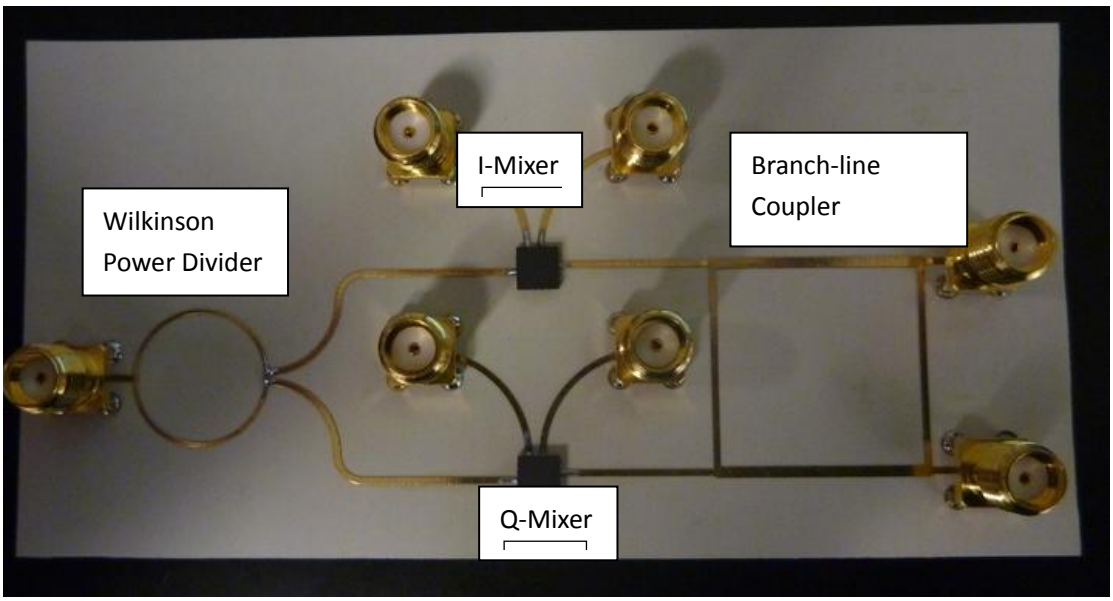

(b)

Figure 4.18 (a): Layout of IQ demodulator, (b): photo of IQ demodulator board

The overall dimension of the PCB is 100mm by 50mm. As seen in Figure 4.18(a), the RF signal injects the board from the Wilkinson power divider and then split equally to feed the RF inputs of I and Q mixers; the LO signal injects from the branch-line coupler and split equally with a 90 degree shift to feed the LO inputs of I and Q mixer. The PCB

was fabricated on the Rogers R3003 substrate, with surface mounted mixers and SMA connectors.

4.3.2 IQ Imbalance Measurement

Quadrature receiver systems designed to produce two orthonormal output signals are used in various applications, including digital communications and Doppler radar. However, the difference between and mixers and signal paths, as well as inaccuracy of the 90 power splitter contributes to phase and amplitude imbalance. Those factors create an undesired linear transform on the input and output signal components, and adversely affect the orthonormal properties assumed for a quadrature system. Thus, the baseband signal for each channel can be expressed as:

$$B_I = A\sin\left(\theta + p(t)\right) \qquad \text{(Eq 4.3)}$$

$$B_Q = A_e A\sin\left(\frac{\pi}{2} + \theta + \emptyset_e + p(t)\right) \qquad \text{(Eq 4.4)}$$

where A_e and $\emptyset_e$ are the amplitude and phase imbalance factors, θ is constant phase delay for the traveling wave, and $p(t)$ is the Doppler modulated signal.

It is possible to correct for a known phase and amplitude imbalance by a simple transformation known as the Gram–Schmidt procedure, which produces two orthonormal vectors.

$$\begin{bmatrix} B_{Iort} \\ B_{Qort} \end{bmatrix} = \begin{bmatrix} 1 & 0 \\ -\tan\emptyset_e & \dfrac{1}{A_e\cos\emptyset_e} \end{bmatrix} \begin{bmatrix} B_I \\ B_Q \end{bmatrix} \qquad \text{(Eq 4.5)}$$

Direct measurement of imbalance factors in such phase modulated systems can be performed through a comparison of output signals resulting from the mixing of two input

signals of different frequency, generated by two synchronized signal generators.

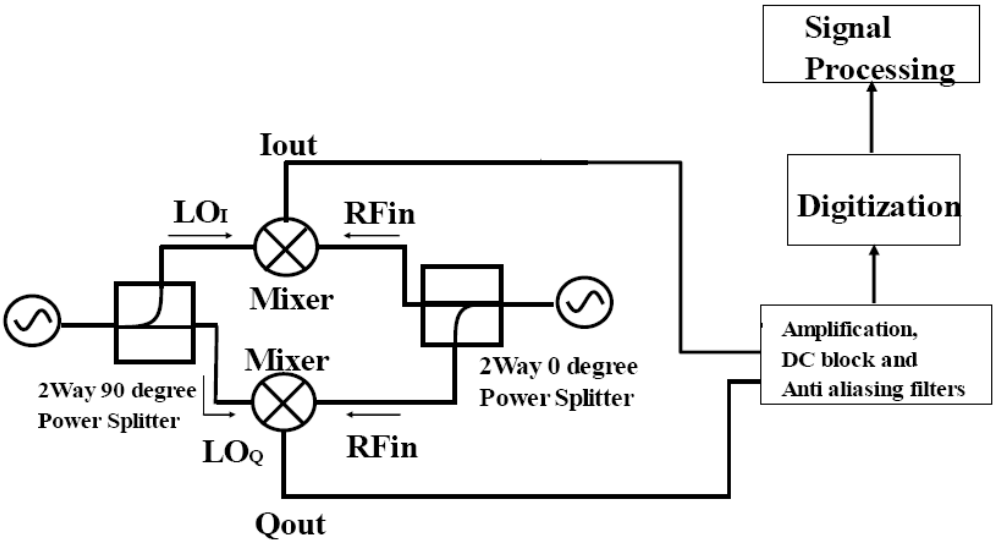

Figure 4.19: IQ imbalance measurement setup diagram

Figure 4.19 shows the block diagram of IQ imbalance measurement setup. Imbalance factor measurements for a quadrature receiver homodyne system can be made by injecting two sinusoidal waves with slightly different frequencies to the LO and RF ports, respectively, using two external sources. HP E4433B signal generator was used at 2.4 GHz with 15dBm output power for LO port. For the RF port, HP 83640B signal generator was used at 2.400002 GHz with -5 dBm output power. The baseband output signals were combined as A-B (IF1-IF2) mode amplified by a gain of 500 and filtered from 0.3 to 10 KHz with Stanford Research SR560 LNAs and then digitized with a Tektronix 3014 digital oscilloscope.

By comparing the amplitude and phase delay of and waveforms, the measured amplitude and phase imbalance factors were determined to be 2.6 and 25 degree respectively. The amplitudes were found by subtracting the maximum from the minimum. The phase difference was found by the peak of the cross correlation between the two signals.

4.3.3 Motion Detection

Based on the Doppler radar theory, the velocity of a moving target can be determined by the phase shift of the received signal. The Doppler measurement will be used as performance test of the IQ demodulator.

The measurement setup is shown in Figure 4.20. The external signal source (HP E4433B) was set at 2.4GHz with 15 dBm power. The signal was split by a 2 way 0 degree power splitter (Mini Circuit ZFSC-2-2500S) to provide the RF output signal to the transmit antenna (ASPPT2988 2.4-GHz ISM-band patch antenna), and LO input power to the IQ demodulator. There is a variable attenuator connected between the power splitter and transmit antenna, which is used for testing the lowest transmit power for the IQ demodulator. The target object is set at the front of the antennas, moving forward and backward about 1.5cm in a fixed frequency 0.2 Hz corresponding to simulated respiratory signal of 12 beats per minute. The picture of the artificial target was shown in figure 4.21. The received signal is sent back from the receive antenna (ASPPT2988 2.4-GHz ISM-band patch antenna) to the RF port of IQ demodulator. The IF outputs signals from the I and Q mixers are AC coupled and amplified by 500 through LNA (Stanford Research Systems SR560).

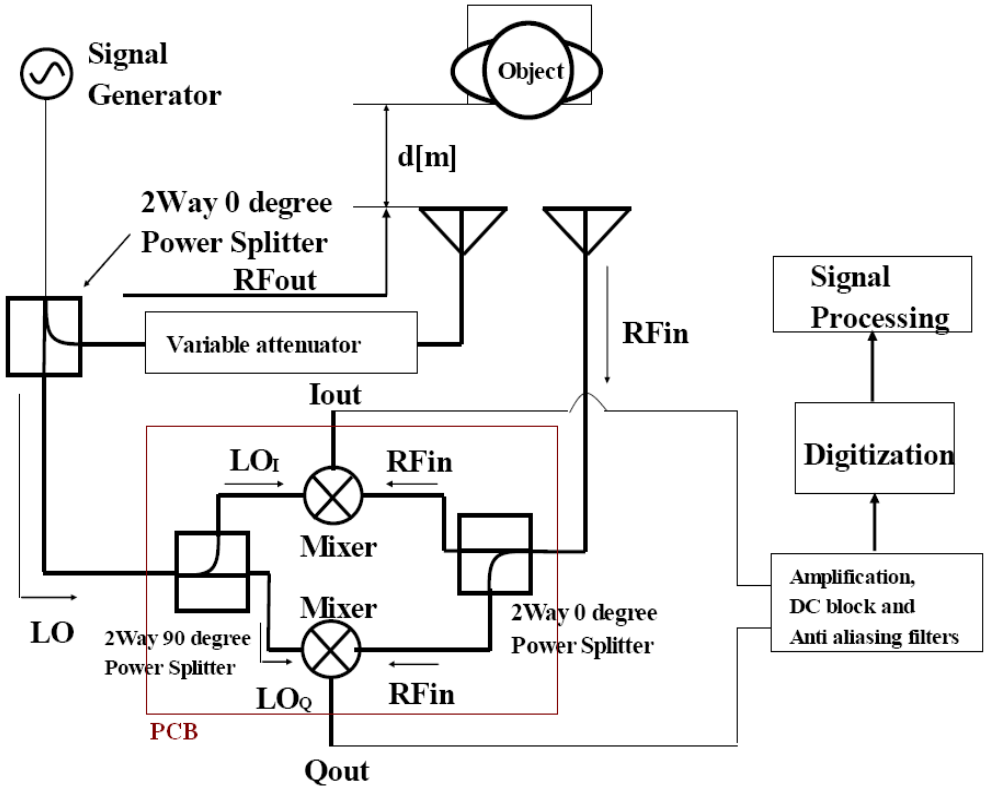

Figure 4.20: Measurement Setup for Doppler Radar

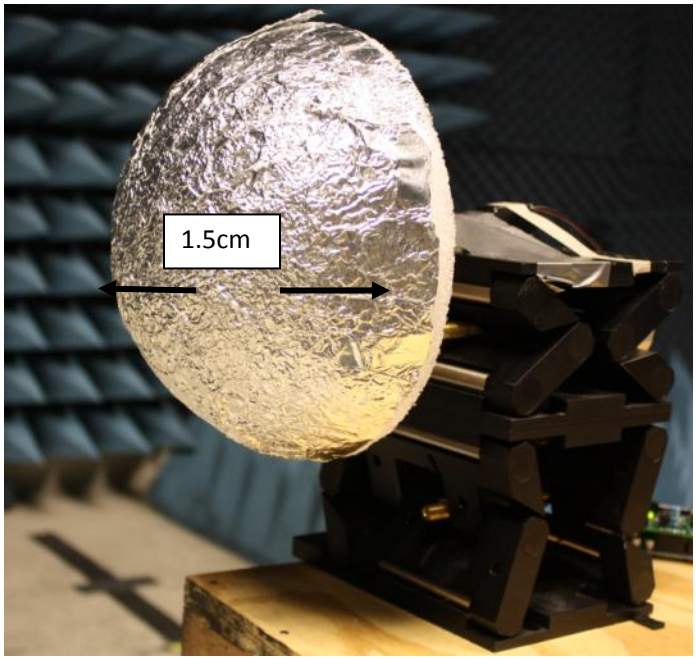

Figure 4.21: Artificial Target Moving at 0.2 Hz

The measurements were taken for various distances from target to antenna and various transmit power level. The Figure 4.22 contains three measurement results. When the distance from target to the antenna is 1 meter without any attenuation, the IQ board

detected the target movement well. Due to the limitation of the room area, the longest distance can be set at 2.5 m from the target to the antenna. In this case, according to the measurement result, the detection is accuracy as well. The transmit power can be varied by the attenuator. The IQ board can handle less 30dB attenuation which promises a acceptable detection result.

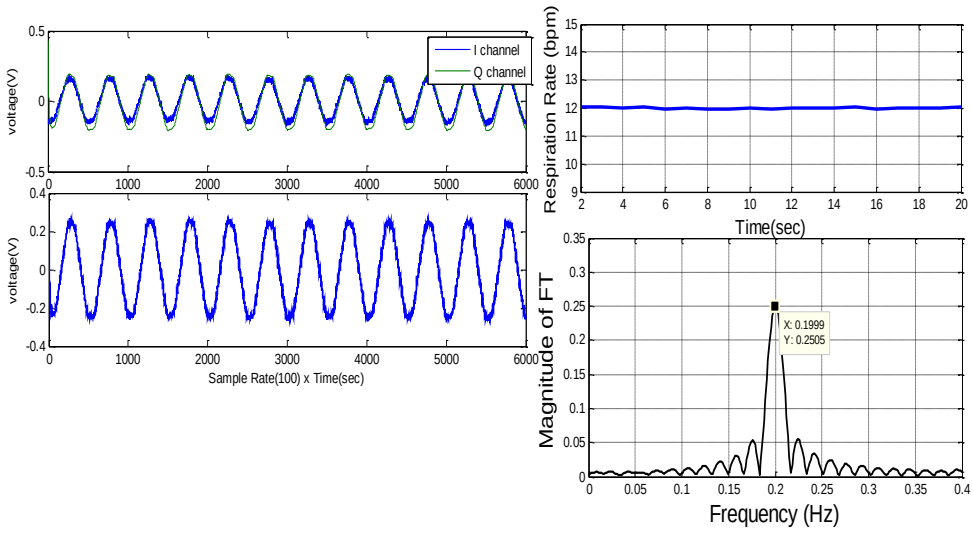

(a) Measurement Result for distance at 1 meter without attenuation

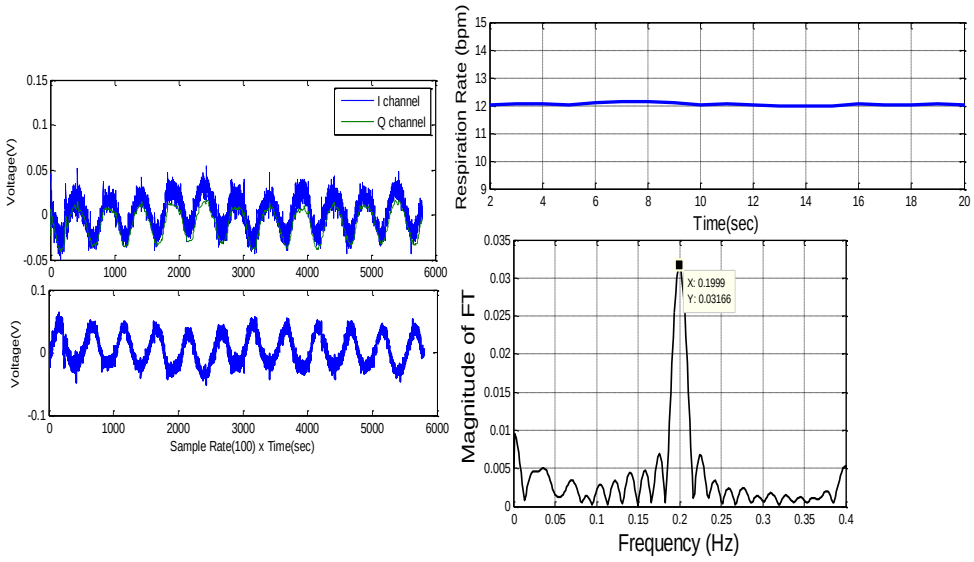

(b) Measurement Result for distance at 2.5 meter without attenuation

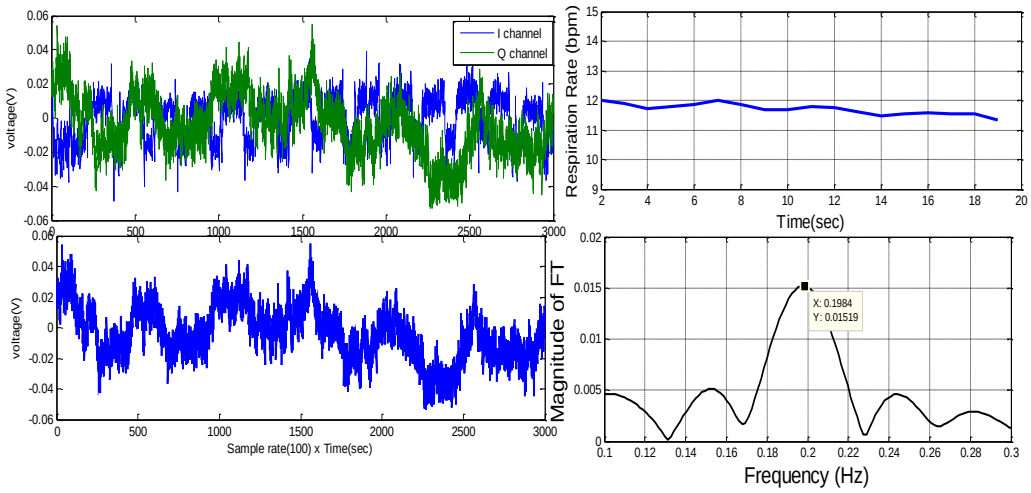

(c) Measurement Result for distance at 1 meter with 30dB attenuation

Figure 4.22: Measured Result of Artificial Target

CHAPTER 5.

DC COUPLED RADAR MEASURMENTS

Direct-conversion trasceivers are commonly used in wireless communications to avoid image rejection filters, and enable higher level of integration with lower power dissipation. These advantages have fueled interest in direct conversion architecture for microwave Doppler-radar of non-contact cardiopulmonary monitoring. However, there are challenges in direct conversion systems. Performance limitations typically stem from quadrature channel imbalance, LO leakage, Flicker noise, and DC offset at the receiver output. The most serious problem is the generation of a DC offset in baseband section following the mixer. The DC offset arises from many causes: the largest offset typically comes from a signal at the LO frequency that is not the desired signal. In communication receivers there is no transmitted signal, so that the offending offset is usually caused by LO coupling to the RF input port. This may happen by the LO signal exiting through the antenna, reflecting off an object, and returning to the receiver through the RF input port, or by the LO coupling to the RF input through the chip substrate, the bond wires, or the package leads. When this signal is mixed to baseband, it may cause a dc offset. Additionally, a large undesired interfering signal at the RF input can leak into the LO port of the mixer, causing additional down-conversion to DC. This DC offset results in Flicker noise which limits system sensitivity. In addition, LO leakage at the antenna end in receiver configurations may cause interference. In this chapter, the LO leakage and the DC offset are measured for two quadrature system as comparison. Due to the less DC

offset in the PCB configuration, the output signals can be DC coupled, without saturating the LNAs.

5.1 Mixer LO-RF Isolation

Mixers are used to transform signals in one spectrum range to some other spectrum range. In radar transmitters, mixers are used to transform intermediate frequency (IF) signals produced by the waveform generator into RF signals. This process is called up-conversion. In radar receivers, the opposite operation is performed. RF signals are down-converted into IF.

The mixer on board need to have high linearity, and high LO to RF isolation. A mixer with balanced structure has high LO to RF isolation, which suppresses both the down-conversion of LO amplitude noise and self-mixing, which leads to a dc current that causes 1/f noise generation. Baseband 1/f noise created by the mixer can be a dominant noise source for Doppler radar which will degrade the sensitivity of the system. If the DC offset can be suppressed, the sensitivity of the system can be improved. Passive mixers exhibit significant lower Flicker noise compared to active mixers due to the fact that there is no dc current, and are often used in direct down-conversion receivers for that reason.

The double balanced passive mixer which is mounted on the radar board has been tested in Cascade probe station. The IP3 is 13.4dBm at operating RF frequency, and the LO-RF isolation is achieved to -52.4dB at 2.4GHz. For the following measurement

comparison, a coaxial quadrature radar system is built. The LO to RF isolation of the coaxial mixer (mini circuit ZFM4212) was measured as -22 dB at 2.4 GHz.

5.2 LO Leakage

As described above, the high LO to RF isolation will suppress the DC offset in the radar system which will improve the sensitivity of the system. In the two antenna configuration in Fig5.1, the LO leakage from the mixer RF port is a main source. The other leakage can be happed due to the imperfection of the hardware such as LO leakage through the substrate, bonding wires and even package leads.

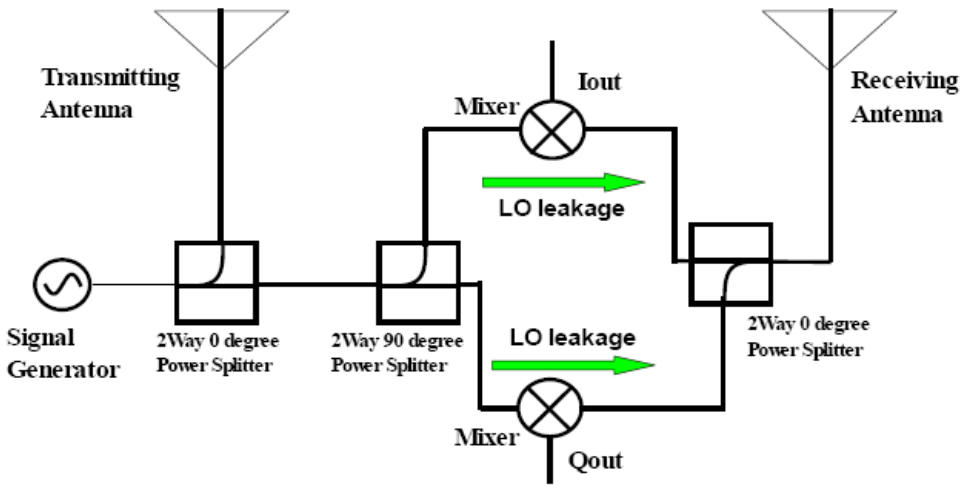

Figure 5.1 LO Signal Leakage in Multiple Antenna System

The LO leakage for the radar receiver system was measured using the setup in Figure 6.2. The coaxial radar system was built and measured for comparison. The coaxial quaduature radar system consists of two mixers (mini circuit ZFM4212), one two way 90 degree power splitter (mini circuit ZX10Q-2-27), and a 2 way 0 degree power splitter

(mini circuit ZFSC-2-2500). From the signal generator, 0dBm input signal was provided to the LO port of the receiver. The spectrum analyzer is connected at the RF input port to measure the LO leakage.

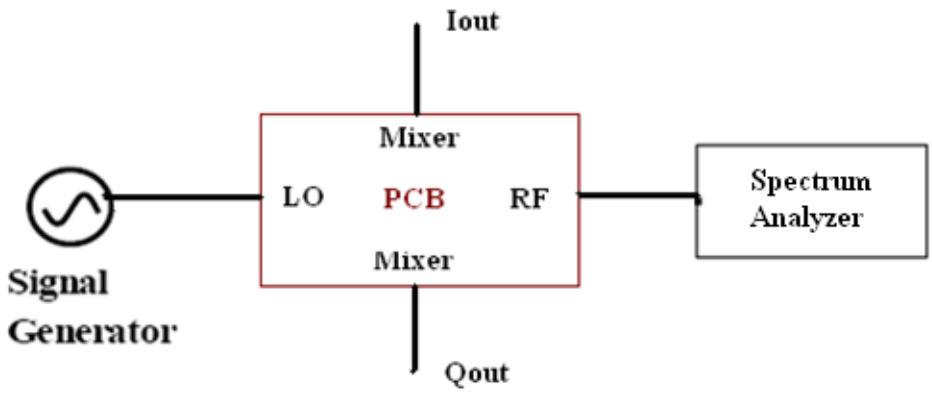

(a) PCB Configuration set-up

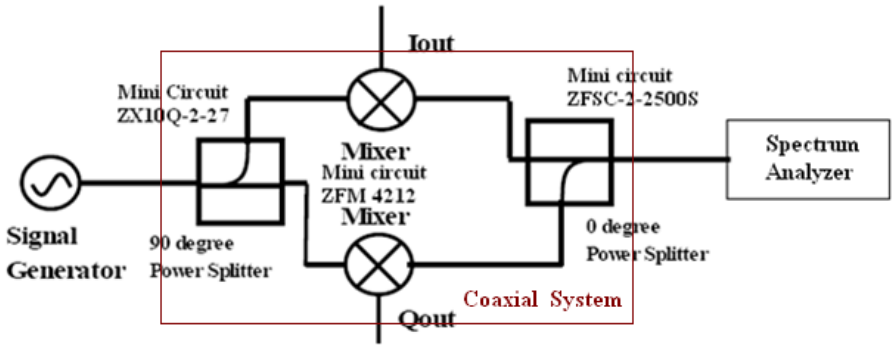

(b) Coaxial Configuration set-up

Figure 5.2 LO Leakage Measurement Setup

The table 5.1 shows the measurement results for the LO leakage power. For the coaxial system, the LO leakage power is -30 dBm; and for the PCB system, the LO leakage power is -45.3 dBm. LO Leakage in the PCB system is over 15 dB lower than in the coaxial system.

Table 5.1 LO Leakage from Mixers Measurement Results Table 1

	Coaxial	PCB
LO Input (dBm)	0	0
LO Leakage(dBm)	-30	-45.3

5.3 DC offset Measurement

The imperfections in circuit components and reflections from stationary objects will cause the DC offset in the radar system. For the hardware imperfection, the mixer LO to RF isolation will result in self-mixing which produces a dc output. The DC offset caused by hardware imperfection is measured for the PCB and coaxial radar receiver system. The measurement set up is shown in Figure 5.3. From the signal generator, the input signal is split by a 2 way 0 degree power splitter (mini circuit ZX10Q-2-27) with one port is terminated by a 50 ohm terminator, and the other port is connected with the LO input port of the radar receiver. The RF input port of the radar receiver is terminated by a 50 ohm terminator as well. The IF outputs from I and Q mixers are connected in LNA with a 30 Hz low pass filter. The signals were not amplified (gain is 1). The DC offset in each channel was read in the oscilloscope.

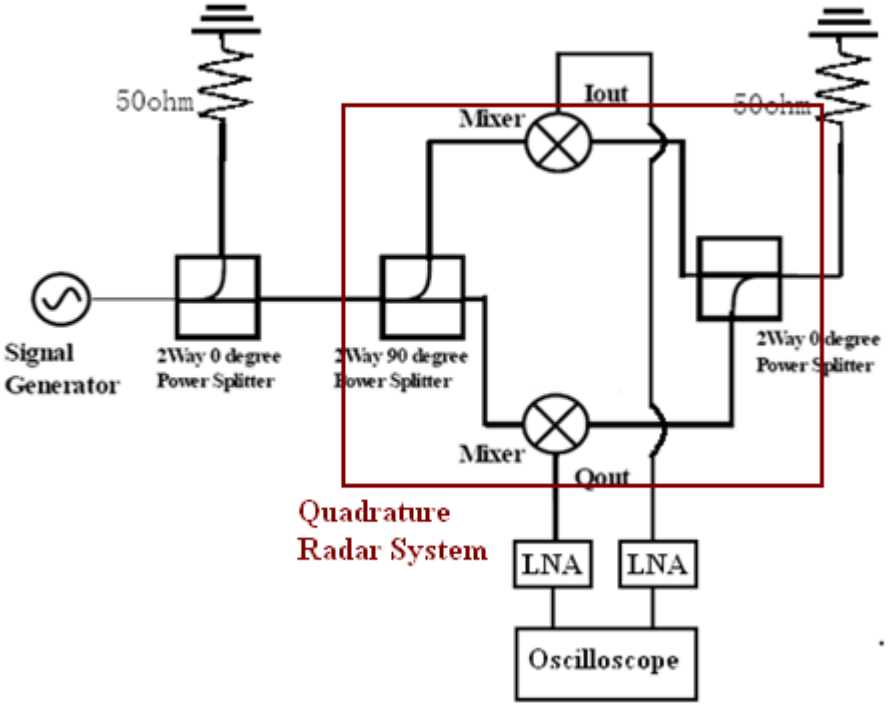

Figure 5.3: DC Offset Caused by Hardware Measurement Setup

From the signal generator, the output signal power level was changed from 15 dBm to 10 dBm stepped by 1 dBm. The signal power to the board was measured by spectrum analyzer. The table 5.2 shows the input power measured at the LO port of the radar receiver and estimated LO power to the mixer.

Table 5.2 LO Power Measurement Results

Input Power from SG	15	14	13	12	11	10
LO to Board by SA	9.4	8.3	7.2	6.2	5.2	4.2
LO to Mixer Estimated	6.4	5.3	4.2	3.2	2.2	1.2

The DC offsets were measured at the different power level for both PCB and coaxial systems. The Figure 5.4 is the DC offset plots for I and Q channel of PCB and coaxial system. The DC offset in each channel is decreased as the LO power drops. Due to the lower LO leakage in the PCB system, the DC offsets in each channel are significantly lower as compared to the coaxial system at different LO input power levels.

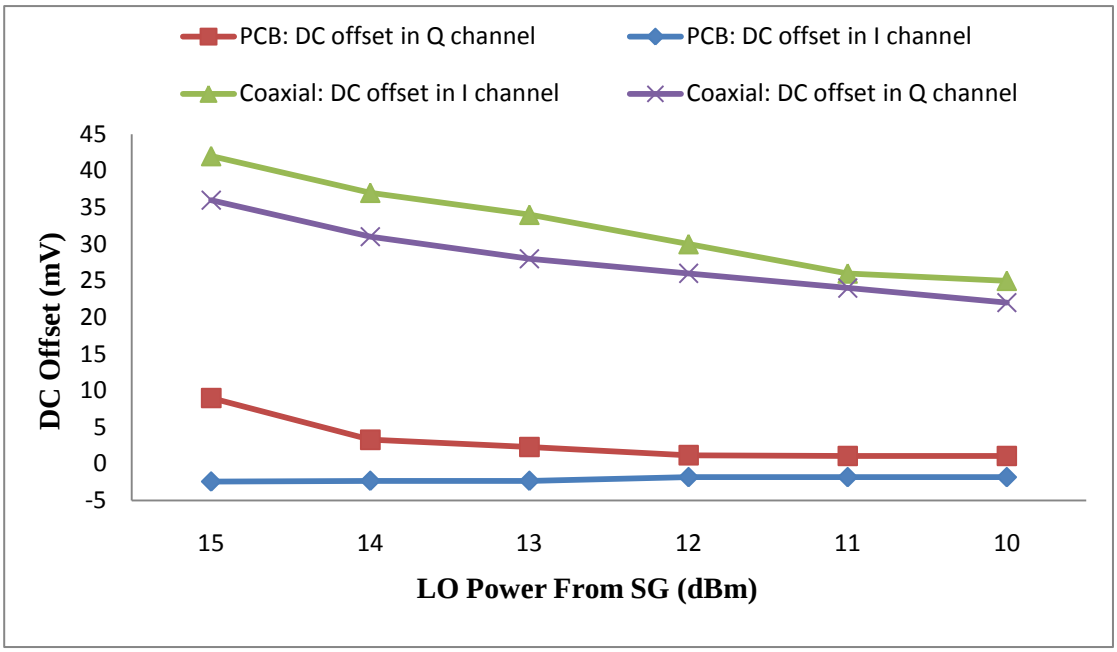

Figure 5.4 DC Offset Caused by Hardware Measurement Result

The clutter reflection can be the other source for DC offset. The Figure 5.5 shows the measurement set-up for the DC offset caused by the clutter reflection. A power supply was used for cancel the hardware DC offset.

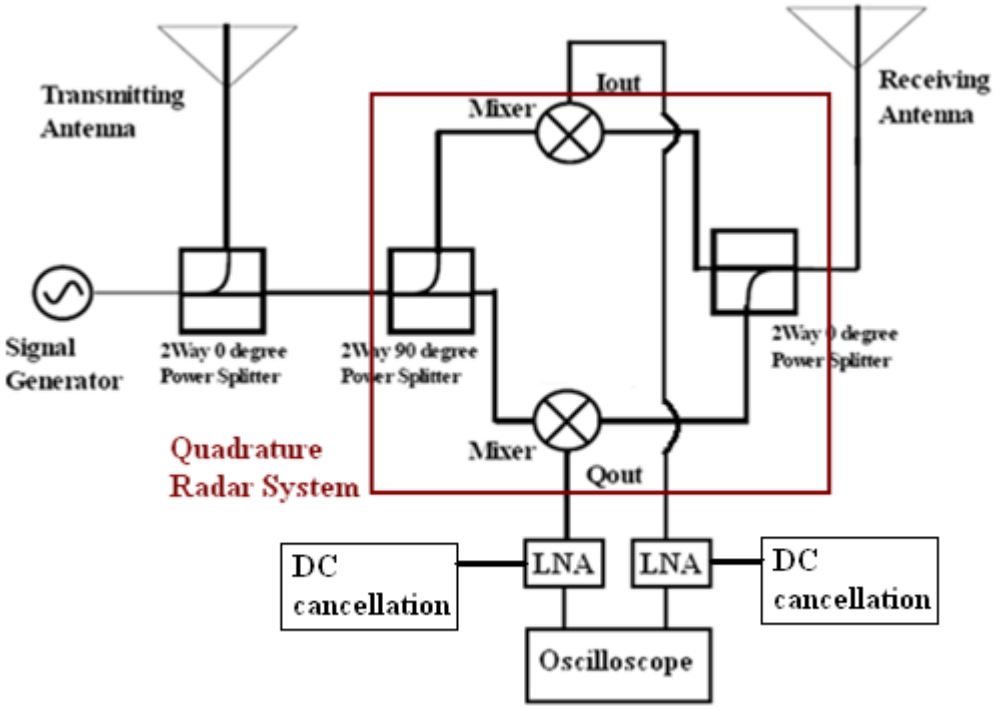

Figure 5.5 DC Offset Caused by Clutter Reflection Measurement Setup

The DC offsets were measured for PCB and coaxial system for different LO power levels. As shown in Figure 5.6, the DC offset in each channel is decreased as the LO power drops. The DC offset in I and Q channel of PCB system is significant lower than in coaxial system below 14 dBm.

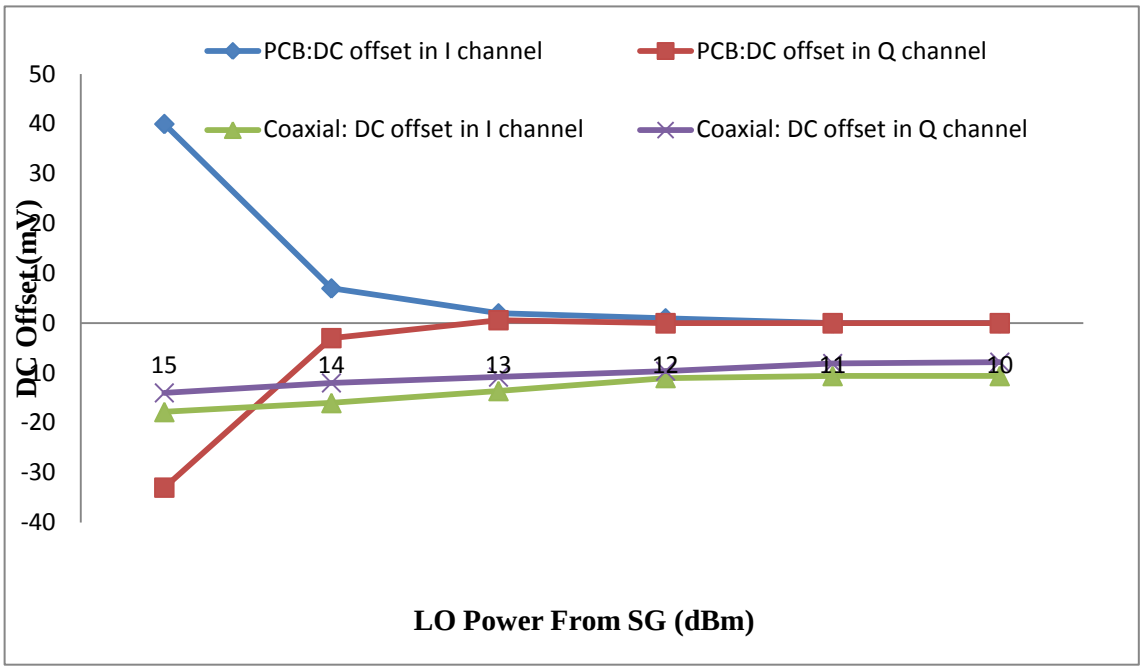

Figure 5.6 DC Offset Cause by Clutter Reflection Measurement Result

The Figure 5.7 shows the measurement set-up for the complete DC offset. The complete DC offs contains the DC offset due to the hardware and also clutter reflection.

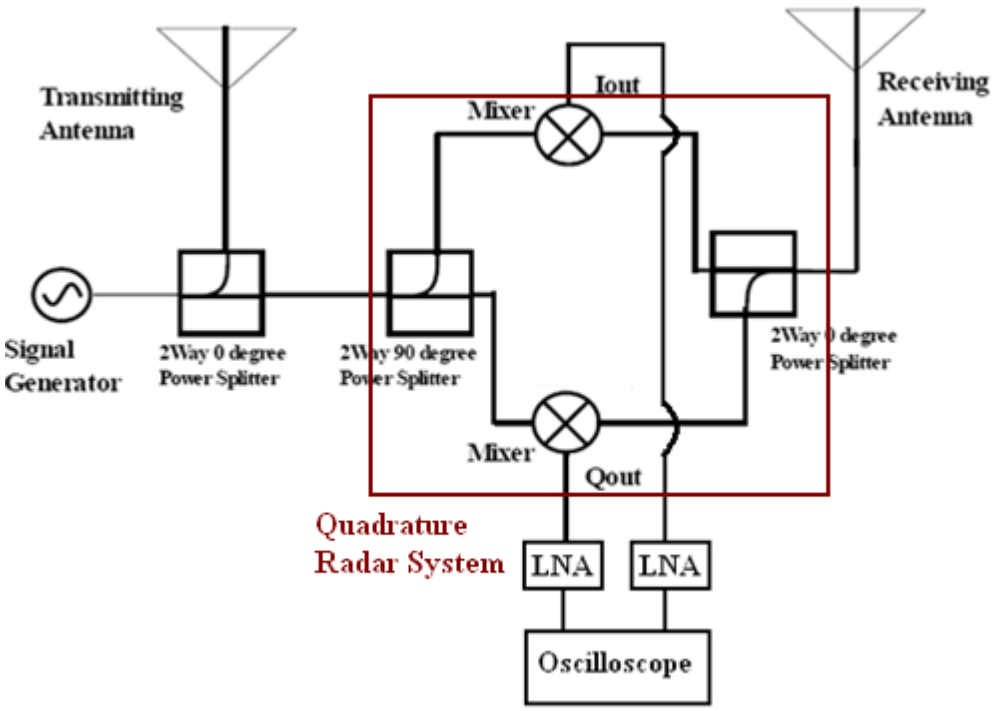

Figure 5.7 Complete DC Offset Measurement Setup

As shown in Figure 5.8, the DC offset in each channel is decreased as the LO power drops. The DC offset in I and Q channel of PCB system is lower than in coaxial system, especially below 15 dBm.

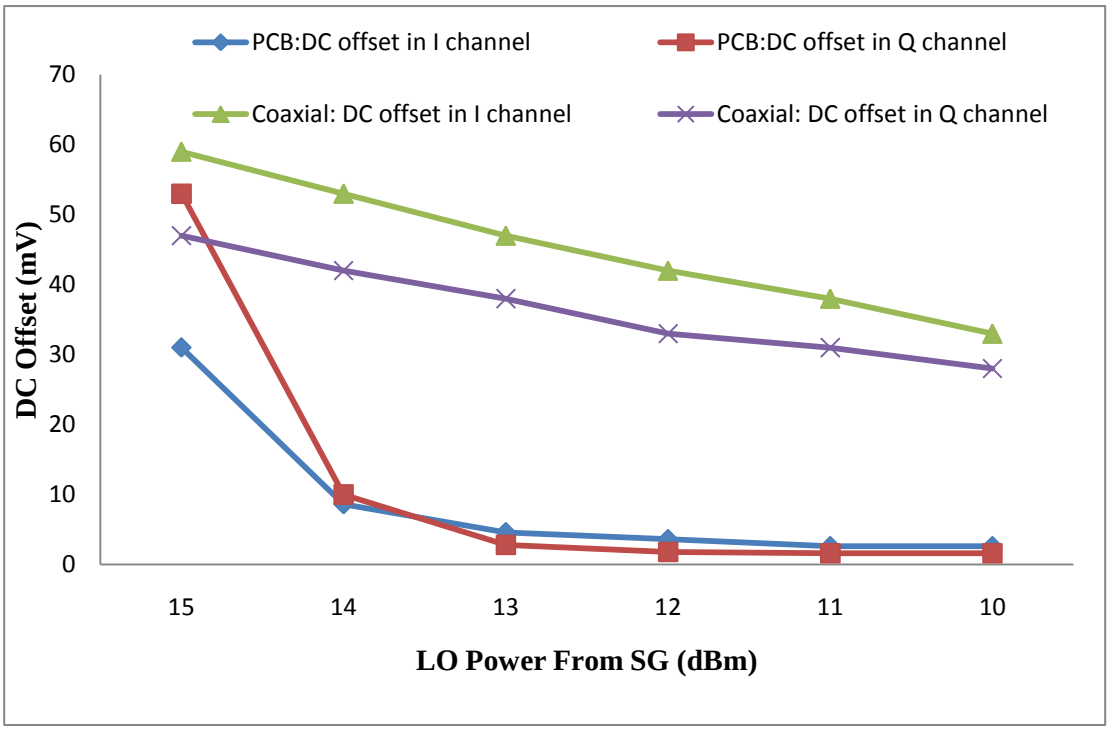

Figure 5.8 DC Offset Cause by Clutter Reflection Measurement Result

From the DC offset measurement results for PCB and coaxial system, the significant lower DC offset achieved at the lower LO power in PCB system.

5.4 DC Coupled Doppler Measurements

In order to remove the undesired DC signals, several DC offset compensation techniques have been proposed for direct-conversion receivers. Typically, the simplest way is AC coupling for the radar output to eliminate larger DC offsets resulting from LO leakage and clutter reflections. This is effective for “motion target indicator” radar, where all clutter results in the unwanted DC signal, and moving targets signatures result in the frequency spectra well above DC. However in Doppler radar physiological monitoring, biological signals occurs at near-DC frequency and are thus difficult to separate from DC components through high pass filtering. On the other hand, AC coupling results in very slow response time, and signal distortion that affects the measurement accuracy.

As measured in the last section, the PCB system exhibits significantly less DC offset compared with the coaxial system at lower LO power level. For the coaxial system, the DC compensation method should be applied to cancel the DC offsets; otherwise the dc component would saturate the amplifier before the target motion signal could be sufficiently amplified for data recording. The set-up of DC compensation is complicated and hard to operate. The PCB system was tested at different LO power level with DC coupled output. When the input power from the signal generation is 14 dBm at 2.4 GHz, the small motion signals were detected with gain of 500 from LNA.

The radar system was built as shown in Figure 5.7. The input power from the signal generator was split to feed the RF out chain and LO input of the radar receiver. The transmitting signal is reflected back from the moving target to the receiving antenna, and then feed to the RF input of the radar receiver.

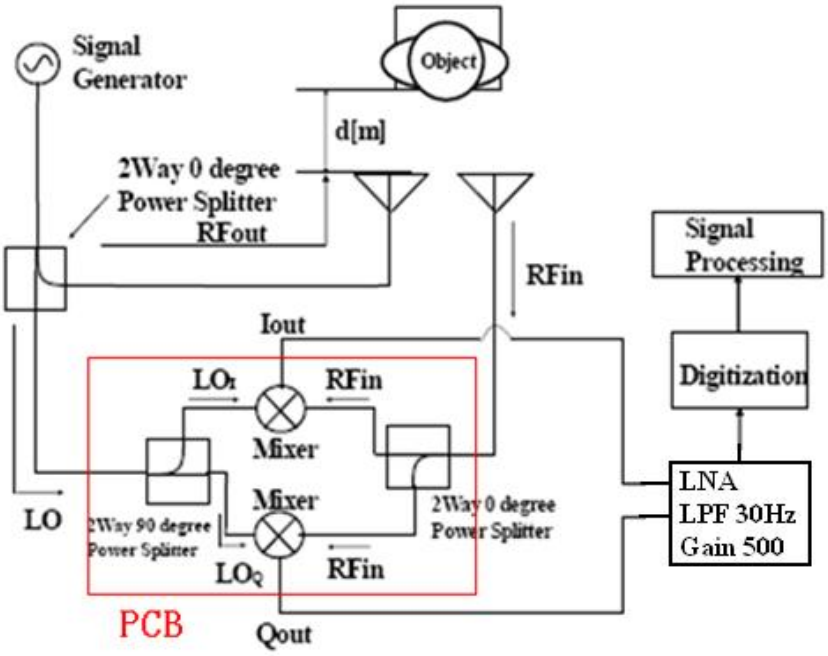

Figure 5.9 DC Coupled Doppler Radar Measurement Setup

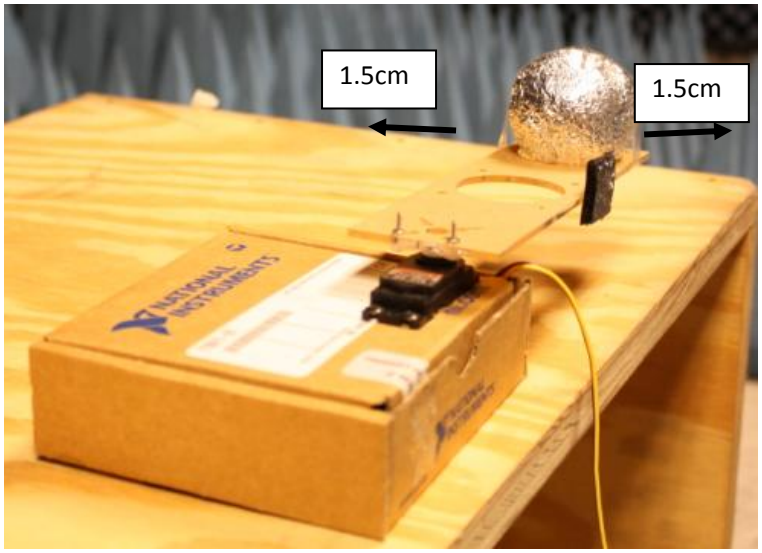

Figure 5.10 Artificial Target Moving at 0.1Hz

The artificial moving target shown in Figure 5.8 is moving forward and backward in about 1.5cm, which generates a 0.1 Hz square wave to simulate the function of holding

breath. The breath rate is 6 (0.1x60) beat per min. The output signals in each channel were DC coupled with the maximum gain before saturation in LNA, and then recorded in DAQ for further signal processing. The DC coupled system was tested under different input power, and the output signals were recorded at the maximum gain for different input power. After analysis in Matlab, the best result was achieved when the input power is 14 dBm from the signal generator, with the maximum gain of 500. The AC coupled data was taken for comparison.

The figure 5.9 shows the original AC coupled and DC coupled baseband signals. The AC coupled data remove all the DC information. The DC coupled data shows the DC offset at each channel.

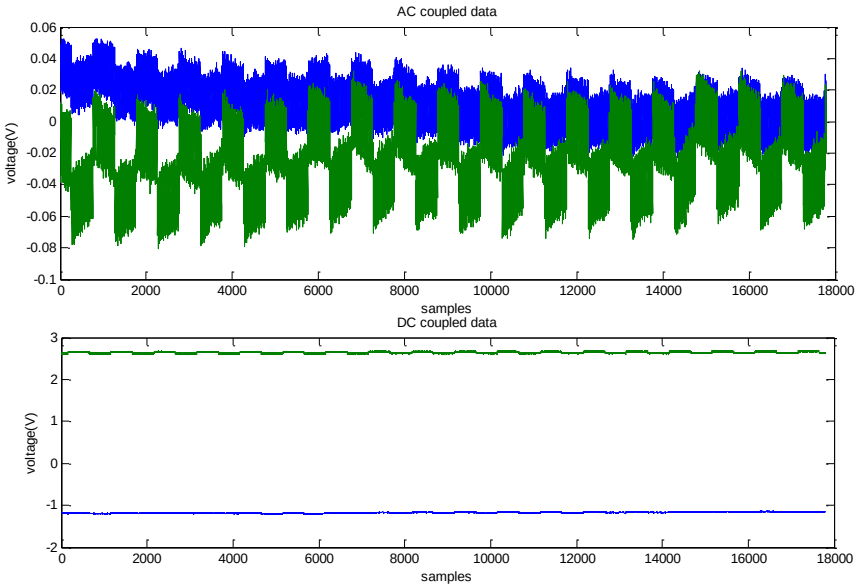

Figure 5.11 Original baseband signals

The linear demodulation is the only way to processing the AC coupled data. But for DC coupled data, either linear or non-linear can be applied. The Figure 5.10 is the comparison for DC and AC coupled data after signal processing. The output for the linear demodulation is proportional to the output power. The output for the non-linear

demodulation is the absolute moving displacement for the target. For the DC coupled data, besides less signal distortion compared with AC coupled data, the absolute displacement can be detected as well.

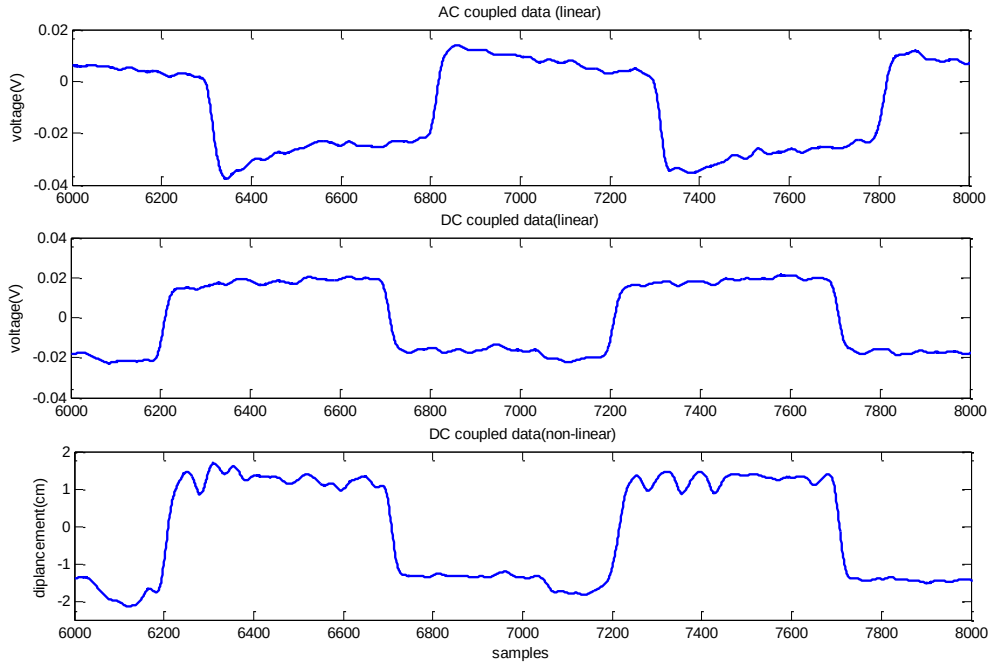

Figure 5.12 Demodulated AC and DC signals

Figure 5.11 is the dected target moving rate for AC and DC coupled signals. And table 5.3 is the data statistic for the mearsurement results. The AC coupled data shows the worst detection accuarcy. For the DC coupled data, the mearsurment result is nearly same. The non-linear demodulation shows a better result compared with the linear demodulation as the less standard deviation.

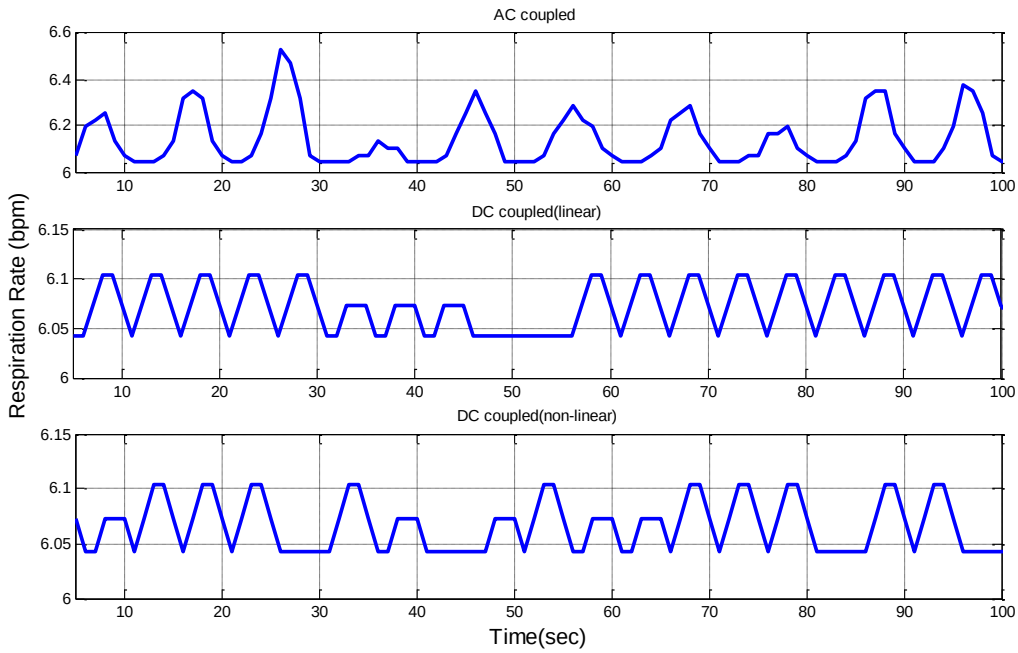

Figure 5.13 Detected moving rate for AC and DC coupled signals

Table 5.3 Measurement results statistics

Moving Rate(bpm)	AC couple	DC couple (linear)	DC coupled (non-linea)
mean	6.142	6.069	6.064
Std	0.1156	0.0256	0.0228

CHAPTER 6

CONCLUSION

The Doppler radar has been used in the monitoring of biological signals of human without any contact. The design of such a system for widespread adoption must offer stable performance and low cost. The goal of this research is to design an I/Q demodulator for the Doppler radar system, to offer small size, low cost, ease of use, and high accuracy.

One of the challenges in Doppler radar systems for physiological monitoring is a large DC offset in the baseband outputs. This DC offset is largely resulting from the parasitic signal leakage between radar ports. Since the physiological signals of interest include frequency content near DC, it is not desirable to simply AC couple radar outputs. While AC coupling effectively removes DC offset, it also introduces a large time delay and distortion. This thesis presented the first DC coupled Doppler radar design and measurements. The DC coupling was achieved by using a mixer with high LO to RF port isolation, resulting in very low radar DC offset, on the order of mW.

In the Doppler radar system, the quadrature (IQ) receiver is used to overcome limitations of a single channel system. PCB power splitter design was used to achieve good signal balance, particularly for the 90 degree splitter. High LO-RF isolation mixer was used to minimize DC offset, and enable DC coupled measurements. In chapter 4, the PCB I/Q demodulator design procedure was described. Based on the theory, the design of

Wilkinson power divider and Branch-line coupler are made in Agilent ADS. The simulation results showed expected performance for both of them. For the Wilkinson power divider, the equal amplitude split and no phase shift of both outputs achieved. For the branch-line coupler, the equal amplitude split and 90 degree phase shift between two outputs achieved. The 2.4GHz resistive ring mixer with on-chip baluns has high linearity and good port to port isolation which is a perfect choice for I/Q demodulator in Doppler radar system. It is packaged in QFN01603 and mounted on the PCB for testing. Finally, the IQ demodulator board is fabricated to integrate the Wilkinson power divider, Branch-line coupler and mixers parts together on the R3003 as substrate. The IQ imbalance was measured for the PCB. The amplitude imbalance factor is determined as 2.6, and the phase imbalance is 25 degree. The IQ demodulator was tested in the radar system to detect the motion of the moving target. The measurement result shows high accuracy of rate of motion for the artificial target.

In chapter 5, DC offset in radar system was analyzed and measured. Two quadrature radar systems were tested for comparison, one is the PCB system, and the other is the coaxial system. Due to the lower LO leakage in the PCB system, significantly lower DC offset was measured for both I and Q channels. The DC coupled signal from the PCB radar system were successfully detected without LAN saturation. The DC coupled and AC coupled data were compared. The DC coupled results show great advantages of less signal distortion and higher accuracy in rate estimation. The benefit can be extended to the human testing which has not been done in this work.

This is the first reported IQ demodulator whose DC offset is small enough to record

DC coupled signals with significant gain, and without any DC cancellation. The measurement results indicate a bright future for avoiding AC coupling in Doppler measurement.

REFERENCES

[1] A. Droitcour, V. M. Lubecke, J. Lin, and O. Boric-Lubecke, “A Microwave Radio for Doppler Radar Sensing of Vital Signs,” IEEE MTT-S International Microwave Symposium, Phoenix, AZ, USA, vol. 1, pp. 175−178, May 2001.

[2] V. M. Lubecke, O. Boric-Lubecke, G. Awater, P.-W. Ong, P. Gammel, R.-H. Yan, and J. C. Lin, “Remote sensing of vital signs with telecommunications signals,” presented at the World Congr. Med. Phys. Biomed. Eng., Chicago, IL, USA, Jul. 2000.

[3] A. D. Droitcour, PhD dissertation, Stanford University, May2006.

[4] A. A. Abidi, “Direct-conversion radio transceiver for digital communications,” IEEE J. Solid-State Circuits, vol. 30, no. 12, pp. 1399-1410, Dec. 1995.

[5] Byung-Kwon Park, Shuhei Yamada, Olga Boric-Lubecke, and Victor Lubecke, “Single- Channel Receiver Limitations in Doppler Radar Measurements of Periodic Motion,” IEEE Radio and Wireless Symposium, San-diego, CA, January 2006.

[6] B.-K. Park, O. Boric-Lubecke, and V. M. Lubecke, “Arctangent demodulation with dc offset compensation in quadrature Doppler radar receiver systems,” IEEE Trans. on Microw. Theory Tech., vol. 55, no. 5, pp. 1073-1079, May 2007.

[7] W. Massagram, V. M. Lubecke, A. Host-Madsten, O. Boric-Lubecke, " Assessment of Heart Rate Variability and Respiratory Sinus Arrythmia via Doppler Radar", IEEE Transactions on Microwave Theory and Techniques, Vol. 57, No. 10, Oct 2009.

[8] C. Song, I. Lo, and O. Boric-Lubecke, "2.4 GHz 0.18μm CMOS Passive Mixer with Integrated Baluns," IMS2009, June 2009.

[9] O. Boric-Lubecke, C. Song,and I. Lo, "0.18μm CMOS Passive Mixer"

[10] Fernando Noriega, Pedro J. González "Designing LC Wilkinson power divider"

[11] "Theoretical Information About Branch-line Couplers"
http://www.ee.bilkent.edu.tr/~microwave/programs/magnetic/bcoupler/theory.htm

[12] B.-K. Park, Alex Vergara, O. Boric-Lubecke, and V. M. Lubecke, "Quadrature Demodulation with DC Cancellation for a Doppler Radar Motion Detector"

[13] A. Vergara, O. Boric-Lubecke, and V. M. Lubecke, "DC Information Preservation for Cardiopulmonary Monitor Utilizing CW Doppler Radar," IEEE EMBS Conference, Vancouver, Canada, August 2008

[14] Z. Zhu and X. Huang, “Gain/phase imbalance and DC offset compensation in quadrature modulators,” IEEE International Circuits and Systems Symposium, 2002, vol. 4, pp. 811-814.

[15] B.-K. Park, S. Yamada, and V. M. Lubecke, “Measurement method for imbalance factors in direct-conversion quadrature radar systems,” IEEE Microw. Wireless Compon. Lett., to be published.

[16] B.-K. Park, Alex Vergara, O. Boric-Lubecke, and V. M. Lubecke, “Signal Coupling and Phase Demodulation Effects on Doppler Radar Heart Signal Extraction”, Oct 2010

[17] Boric-Lubecke Olgaa, Lubecke Victor M.a, Mostafanezhad Isara, Byung-Kwon Parkb, Massagram Wansureec, Jokanović Brankad , “Doppler radar architectures and signal processing for heart rate extraction” Microwave Review 2009, vol. 15, br. 2, str. 12-17

[18] B.-K. Park, V. M. Lubecke, O. B-Lubecke and A. H-Madsen, “Center tracking quadrature demodulation for a Doppler radar motion detector,” IEEE Int. Microw. Sym., June 2007